FINAL REPORT

OZONE UPTAKE IN RELATION TO WATER AVAILABILITY IN PONDEROSA PINE FORESTS: MEASUREMENTS, MODELING, AND REMOTE-SENSING

PMIS #76735

King's Canyon and Yosemite National Parks

Jeanne A. Panek
Panek & Associates Research Consulting
Berkeley, CA

Susan L. Ustin
Center for Spatial Technologies and Remote Sensing (CSTARS)
University of California, Davis, CA

Project Period: January 1, 2002-March 31, 2004

TABLE OF CONTENTS

Abstract

Ozone is a ubiquitous and toxic air pollutant which threatens forest ecosystem health throughout the United States and much of the rest of the industrialized world. To cause injury, ozone must enter leaves through stomatal pores, which open and close under plant control to regulate gas exchange and water loss. High stomatal conductance, and thus high ozone uptake rates, have been shown recently to be strongly correlated with high soil moisture in drought-adapted forest ecosystems such as those in California. Currently little is understood about temporal and spatial variability in stomatal conductance in these systems and how this variability affects ozone uptake, especially in response to the heterogeneous distribution of water across the landscape. In this sense, remote sensing can help in detecting vegetation physiological parameters to place the spatial variability of water stress and physiological conditions and canopy water content into a spatial context.

In this study, physiological response of pine in mesic riparian locations having year-round access to water was compared with response of pine in upslope dry locations which are drought-stressed during the growing season, repeated in 2 locations – Yosemite Valley and King's Canyon, CA. Differences in transpiration and stomatal conductance, and the consequent differences in ozone uptake were measured. Sap velocity techniques were used to measure whole-tree-level responses to changes in soilwater availability. A portable photosynthesis system was used to measure leaf-level response. A physiological model was tested for adequacy in extrapolating to the landscape.

From the "in situ" field studies, while all sites showed a decline in transpiration, stomatal conductance, and ozone uptake over the growing season drought period, the mesic riparian site showed the least decline and thus the greatest ozone uptake of all the sites, as hypothesized. Soil moisture measurements at 50 cm were found to be inadequate at measuring water accessible to pine, because pine can tap into water at greater depths than can be monitored. Water potential measurements showed that the mesic, riparian Yosemite site was the only unstressed site throughout the growing season drought. The riparian site in King's Canyon, although close to the King's River, became drought-stressed by the end of the growing season. Thus close proximity to water is not a useful indicator of year-round access to water. Because of the discrepancy between measured and actual soil water availability, canopy water stress must be assessed by either direct water potential measurement or through remote sensing techniques, not by monitoring soil moisture.

The reduction in stomatal conductance and ozone uptake over the season due to drought stress was significant at the dry upslope sites, but greatest at the King's Canyon site. The effect of drought on the King's Canyon pine was to cause a reduction in ozone uptake of 80-90% over the growing season. The effect of drought on dry upslope Yosemite pine was a reduction in ozone uptake of around 50%.

Total annual ozone uptake at the mesic Yosemite site was 33% greater than the dry upslope site. In the late summer, daily peak ozone uptake at the mesic Yosemite site was 46% higher than uptake at the dry site.

STOMATA, a physiological model of gas exchange developed for Sierra Nevada pine forests, predicted annual and diurnal variability with reasonable accuracy at the Yosemite sites, once soil moisture at the lower site was modified upwards to better

represent actual available soil moisture there. Thus, it can be used as a tool for extrapolating physiological response to drought across the Sierra Nevada.

Remote sensing analyses were conducted using data from NASA's Advanced Visible Infrared Imaging Spectrometer (AVIRIS). Because of the high spectral resolution (224 spectral bands) that was combined with high spatial resolution (~ 4 m pixels) in AVIRIS data we were able to map the location and the physiological conditions of vegetation communities in the two study areas. Unfortunately, due to the difficulty in mapping single species distribution and the insensitivity of other species in the habitat that co-occur with Jeffrey and Ponderosa pines, we could not define a strong correlation between ozone injuries and water stress conditions. However further analyses have been planned to improve the species composition map which may then yield closer correlations between water stress conditions measured in remotely sensed imagery and field measured conditions.

The heterogeneous distribution of water throughout the landscape has a profound effect on spatial patterns of transpiration, stomatal conductance, and ozone uptake of pine forests. Pine with access to permanent water through the summer drought period take up significantly more ozone than pine which have access only to rainfall and snowmelt water. Furthermore, temporal changes in water availability *in situ* caused dramatic physiological response and consequent changes in ozone uptake. This result suggests that changes in timing and amount of snowmelt which are anticipated with predicted changes in climate, will profoundly influence pine physiology, including ozone uptake.

Introduction

Problem: Ozone as an environmental threat to forest ecosystems

Ozone is a ubiquitous and toxic air pollutant which threatens forest ecosystem health throughout the United States (Miller et al. 1996; Skelly et al. 1997; Treshow 1984) and Europe (Matyssek et al. 1997; Rennenberg et al. 1997). Ozone stress first affects photosynthetic systems, needle retention and crown growth, but chronic exposure can lead to changes in forest structure and function. Ozone stress results in decreases in stand growth and vigor, loss of ozone-sensitive tree species, replacement by other species leading to changes in fire-related forest dynamics and changes in forest nutrient cycling. Despite efforts to curb the emissions of precursors which form ozone (NO_x and VOCs), ozone concentrations continue to rise worldwide (Demerjian et al. 1992; Marenco et al. 1994; Stockwell et al. 1997).

Forest ozone injury was reported as early as the 1960's in ponderosa pine (*Pinus ponderosa*) stands in California (Miller et al. 1963). Since then, injury has been well-documented in remote pine forests of southern California (Arbaugh et al. 1998; Bytnerowicz 1996; Grulke 1998; Miller et al. 1996), throughout the Sierra Nevada (Arbaugh et al. 1998; Duriscoe 1987b; Duriscoe 1990; Pronos and Vogler 1981) and in other remote forested areas throughout the US downwind of sources. While ozone pollution in California's urban areas has declined in general over the last 20 years, ozone pollution in remote natural areas has increased (CARB 1999). In 1999 the National Park Service ranked Sequoia National Park among the "worst ozone polluted national parks" in the country (National Park Service 1999). Once created from precursors in transit areas and from industry, ozone is carried by typical air mass trajectories SW through the Central and San Joaquin Valleys, and deflected into the Sierra Nevada at Sequoia and King's Canyon National Park by the transverse Tehachapi range (Figure 1).

To cause injury to trees, ozone must enter leaves through stomatal pores (Darrall 1989; Reich 1987; Runeckles 1992), which open and close under plant control to regulate gas exchange and water loss. The amount of injury which ozone causes depends, in part, on the amount of ozone taken up by foliage, which varies with stomatal conductance. Stomatal conductance generally increases in response to increases in light, soil moisture and atmospheric humidity. In California's drought-stressed pine ecosystems, stomatal conductance is primarily limited by soil moisture, thus ozone uptake in trees is very dependent on soil water availability.

Background

In drought-adapted Mediterranean forest ecosystems such as California, high ozone uptake rates have been recently shown to be decoupled from high ozone concentrations because stomatal aperture is very sensitive to soil moisture. At high soil moistures in the spring and early summer in these systems, stomatal conductance is high and thus ozone uptake is high. When soil moisture drops during the protracted summer drought, conductance drops and ozone uptake decreases. Ambient ozone concentrations are closely tied to temperature, so ozone concentrations tend to rise through the summer. Despite higher ozone concentrations in late summer, ozone uptake can be very low

because of low conductance. The relationships between ambient ozone concentrations, soil moisture and stomatal conductance and their effects on ozone uptake are complex and were elucidated in earlier research (Panek 2004; Panek et al. 2001; Panek and Goldstein 2001; Bauer et al. 2000).

The understanding of ozone effects on intact forest systems is limited to a moderate number of well-documented surveys which have quantified visible foliar injury (Arbaugh et al. 1998; Duriscoe 1990; Miller et al. 1996; Pronos and Vogler 1981). These studies have limited their approach to linking visible injury with ambient ozone concentrations, not uptake. Most studies have avoided the more complex task of understanding the physiological mechanisms which may limit the uptake of ozone into foliage. Our work is among the few studies to include physiological controls on ozone uptake in intact forests (the other two are: Grulke 1998; Patterson and Rundel 1990). Clarifying mechanisms is the only way to understand the relationship between cause (ozone stress) and effect (antioxidant synthesis, chlorotic mottling, growth declines, etc.), to understand the magnitude and the meaning of residuals in the correlation, and to use that understanding to develop methods to monitor forests and aid in management practices.

There is evidence that trees in drought-adapted ecosystems with year-round access to water are more vulnerable to injury from extant ozone concentrations than trees which experience the typical summer drought. A watering experiment of *in situ* ponderosa pine showed that trees with access to soil water through the summer retained high stomatal conductances and took up 35% more ozone and carbon than controls, even in a relatively wet El Niño year (Panek and Goldstein 2001). Re-examination of results from survey plots of ozone injury in Yosemite and Sequoia/King's Canyon supports this hypothesis: plots in riparian zones tend to have more ozone injury that upslope plots (Duriscoe and Stolte 1989).

Specific objectives addressed in this study

The strong interaction between soil moisture and ozone uptake is beginning to receive significant attention as drought-adapted forest ecosystems, with ecologically and economically important tree species, are becoming increasing affected by poor air quality. Ozone uptake rates are likely to be highly heterogeneous across the landscape due to spatial and temporal heterogeneity of water availability (rivers, streams, and snowmelt), but this is currently unknown because ozone uptake has never been measured at the landscape scale. We sought a more in-depth understanding of the interaction between water availability, canopy conductance and ozone uptake that was scaleable to the landscape with the help of remote-sensing techniques. We investigated contrasting soil moisture regimes - trees with and without summertime access to water - to elucidate physiological response to water availability, in terms of carbon uptake, transpirational losses, canopy conductance and ozone uptake. Mechanistic response in photosynthetic pathways which function to capture light and reduce carbon were contrasted in wet and dry environments.

Furthermore, we initiated the development of a method which combined recent advancements in modeling stomatal conductance with novel methods of remotely estimating forest canopy water content to estimate canopy conductance in broad forested areas. The research conducted by Ustin and Curtiss (1989) on the spectral characteristics

of ozone-treated conifers showed that ponderosa pine responds spectrally to an increase in ozone exposures, through a significantly higher reflectance across the visible and shortwave-infared regions of the spectrum and a decrease in reflectance across the near-infared. These spectral changes are indicative of a reduction in the leaf chlorophyll content. In the years since this study, it has become possible to quantify the concentration of pigments and water content from spectra at the field scale and in imagery of larger regions.

Combined with extant methods for assessing ozone concentrations across broad regions of the landscape (passive monitors, eg.), we hope to further develop this new approach to provide the much-needed assessment of ozone uptake rates at the landscape scale (Ustin: Determination of Ecosystem Patterns in Sequoia/Kings Canyon National Park Using Hyperspectral Remote Sensing, submitted to NPS).

Methods

Site Locations

Sites were established in Yosemite and Kings Canyon National Parks, with the help of the Park Service research staff, to utilize existing moisture gradients away from a riparian zone within Yosemite Valley and Kings Canyon. The gradient allowed us to observe forest gas exchange before and after the summer drought in trees with continuous access to water (riparian wet area) and trees which go dormant in response to the soil drought (upslope dry area). Figure 2.

Yellow pine in both Yosemite Valley, and King's Canyon have been sampled for ozone injury (Duriscoe 1987a; Duriscoe 1987b; Duriscoe 1990). In Yosemite, mean chlorotic mottle for the Merced River drainage was 0.17 (slight injury, index exponential from 0-3), with 26.9% of trees showing visible injury. Mean chlorotic mottle for the south fork of the King's river was 0.14 with 26.7% of trees showing injury (Duriscoe 1990).

Two 40 x 40m plots were established in the vicinity of sites where injury was measured, in Yosemite Valley (ponderosa pine) and in King's Canyon (Jeffrey pine). Instrumented trees (detailed below) were at the center of the plot. One plot was in each of the moisture regimes, in each of the parks for a total of 4 sites: Upper Yosemite (dry), Lower Yosemite (wet), Upper King's Canyon (dry), Lower King's Canyon (wet). A creek was observed near each of the upper sites, the flow of which was greatly affected by season. The Yosemite creek dried up in the summer, however the King's Canyon creek did not. Site maps, Figure 3.

To investigate the remote sensing the physiological responses of Jeffrey Pine and Ponderosa Pine to the ozone injuries, and to contrast these findings with soil moisture availability, AVIRIS data was acquired on 2 October 2002, at or after the end of the dry summer season. The Twin Otter plane was flown at an altitude to produce pixel resolutions of approximately 4m x 4m. Data was provided in radiance format which we calibrated to apparent surface reflectance using the ACORN radiative transfer model. Additionally, the data were provided in a geo-corrected format based on the onboard GPS and navigation information. Subsequent geographical correction was performed using a USGS Orthophoto data to correct the geolocation. As illustrated in Figure 4 and Figure 5

the flight lines covered the Yosemite Valley along the Merced River and the Kings Canyon valley along the Kings River.

Instrumenting the sites

Ozone

The National Parks installed and maintained ozone monitors for the duration of the project near each of the sites. SEKI installed a low-power active ozone monitor (2B Technologies, Boulder, CO) which used solar panel/battery power at Cedar Grove on June 14, 2002 to capture diurnal variation in ozone concentration in the upper King's Canyon (Hassan Basagic, Annie Esperanza). Ozone values were sampled every 10 seconds and stored as 5-minute averages in the non-winter season when the instrument was accessible. In the winter, when the road to the site was closed, data was stored as hourly averages. Gaps in data were filled using the relationship between ozone, temperature, and radiation during the operable hours determined from 1.5 years of operation (R^2=0.43, P<0.0001).

$$Ozone\ (ppb) = 1.49\ T_{air}\ (\text{ºC}) + 0.006\ PAR\ (W\ m^{-2}) + 8.27 \qquad\qquad Eq.\ 1$$

This fit was the best of several methods of gap-filling explored, including using Cedar Grove 2002 data to fill in 2003 gaps (R^2=0.28), and using Grant Grove ozone data averaged from 1990-1995 (R^2=0.27). Passive ozone monitors were run at Cedar Grove and Road's End, sampled weekly over the growing season. Passive data are found at:
http://www2.nature.nps.gov/air/Studies/passives.cfm
The data labeled CEDAR GROVE is the filter at Road's End, CEDAR GROVE 2 is the filter at Cedar Grove.

Yosemite National Park (Katy Warner, John Ray) put both one active and two passive ozone monitors in Yosemite Valley from 2002-2003. The active monitor (TECO 49C, Thermo Electron Corporation, Franklin, MA) was installed near Sentinel Bridge. Gaps in data were filled with ozone data from Turtleback Dome (37.71º N, 119.70º W), corrected for site using relationships from passive data (see Results section). The passive monitors were sample weekly over the growing season (Katy Warner). YOSE10 is the passive at Turtleback Dome, YOSE14 at El Cap Meadow (the lower site), and YOSE15 at the wood yard (upper site).

In addition, meteorological variables were monitored at each of the 4 sites continuously from May 2002 through November 2003 - soil moisture, RH, leaf wetness, PAR, T_{soil}, T_{air}, and T_{leaf} .

Sap flow measurements

Three canopy trees at each site were instrumented with sap flow sensors. Trees were selected to be in the general area of previous ozone injury assessment research, to be within 45-67 cm DBH, and to be within 10 m of each other, so that one datalogger could run all instruments. Sap flow was monitored using the heat-ratio method (Burgess et al. 2001), a method employed and further developed by M. Kurpius for her doctoral work and described below (Kurpius et al. 2003). Units comprising two thermistor probes and one heater probe were inserted radially into the sapwood of emergent pine trees at 8 m

above the ground. For each sensor set, a thermistor probe was placed 6 mm above and 6 mm below the heater probe and a 30 cm wide collar of reflective insulation was be placed around the stem to prevent direct solar radiation on the exposed portions of the sensors. Eight sensor sets were deployed on 3 trees–aspects SE,SW,N on 2 trees and N,S on 1 tree. The trees instrumented were chosen to be similar across sites and representative of the size distribution of emergent trees in the stand. Cores were taken in May to determine sapwood fresh weight, sapwood oven-dried weight, water content and wood volume. Corrections were applied, using the method of Kurpius et al. (2003) for: probe misalignment, adjustment for correct thermal diffusivity (Becker and Edwards 1999), wound effects, and radial and circumferential variation in rates of sapflow (Burgess et al. 2001). Further, the sap velocity measurements were adjusted to account for volumetric wood and water contents (Hatton et al. 1995). Stand transpiration (E mm h^{-1} or mm day^{-1}) was estimated from E = J x S, where J is the sap flux density (mm^3 mm^{-2} h^{-1}) and S is the cross-sectional sapwood area per ground area (m^2 m^{-2}). Sap flux density is the mean sapflow averaged by the mean sapwood area (see Clearwater et al. 1999; Granier and Loustau 1994; Teixeira Filho et al. 1998). Tree canopy conductance from the sap velocity measurements, g_c, was calculated based on (Monteith and Unsworth 1990; Phillips and Oren 1998) with the modification of neglecting aerodynamic conductance:

$$g_c = \frac{\gamma \cdot \lambda \cdot E}{C_p \cdot \rho \cdot D} ,$$ Eq. 2

where γ is the psychrometric constant, λ is the latent heat of vaporization of air, E is the transpiration rate, C_p is the specific heat of air, ρ is density of air, and D is the vapor pressure deficit of the canopy air. This approximation is valid when aerodynamic resistance is much smaller than canopy resistance as is generally the case in open coniferous stands such as these (Gates 1968; McNaughton and Jarvis 1983; Oren et al. 1998).

Other measurements at the sites

Leaf area index was estimated using the sapwood area method (Marshall and Waring 1986) and published allometric relationships to estimate foliar biomass (Gholz et al, 1979). Site specific leaf area data was then used to determine leaf area per tree, and then summed to determine leaf area of the entire plot. Tree diameter at breast height (DBH) of all trees within the plot was measured. Leaf area index was calculated from the pine diameters only.

Physiological and phenological measurements were made in May and August to contrast physiology and growth under well-watered conditions with that under drought-stressed conditions. Three trees with south-facing branches close to the ground were selected at each site. Needle length, candle length, and specific leaf area were measured at all of the sites. Predawn and afternoon water potential measurements were made (Pressure Chamber, PMS Instruments, Corvallis, OR) for direct determination of canopy leaf-water status. Leaf-level physiology measurements were made once in May when all trees were well-watered and once in August when upslope trees were drought-stressed, using a LiCor 6400 portable gas exchange system (LiCor Instruments, Lincoln, NE), on 3 trees with south-facing, sun-exposed branches close to the ground. Physiological

measurements included 1) a one-day time-series capturing the diurnal pattern of conductance, transpiration and photosynthesis, 2) photosynthetic response curves (A/Ci and AI) to determine maximum rate of carboxylation (V_{max}), maximum rates of electron transport (J_{max}), and respiration rates (R_d), quantum efficiency and light compensation points. These measurements were made with an eight-minute stabilization period with each change in chamber conditions (L. Xu, pers. comm.). These values were important for parameterizing mechanistic models of gas exchange (eg. STOMATA) and also provide insight into mechanistic response of trees to drought.

Ozone damage was measured on one branch from each of the trees on which leaf-level physiology was measured, using the method of Miller et al. (1996).

Modeling

Meteorological data measured at each site was used to run a physiological model, STOMATA, developed by Misson et al. (2004) for ponderosa pine data across a north-south transect in the Sierra Nevada. The model is a leaf-level model that uses a Farquhar/Ball-Berry approach to estimate stomatal conductance and photosynthesis. The approach has been developed on dryslope ponderosa pine, and uses a special function for water stress that modifies the standard equations based on soil moisture, thus the model is very sensitive to soil moisture. For model details, see Misson et al. (2004).

Remote Sensing Analysis

In order to analyze the images for the detection of the chlorophyll and water canopy content, primary the following image processing were performed:
- Mosaicing
- Atmospheric calibration
- Georectification
- Vegetation classification

Mosaicing

The flight lines, for Yosemite Valley and for Kings River Valley were delivered in 3 different image scenes (standard units of image data that correspond to 512 pixels by 620 lines). In order to have a complete overview of the two study areas the scenes were mosaicked using the pixel based method. Figures 4 and 5 show the mosaic of the two flightlines.

Atmospheric calibration

The atmosphere plays an important role in the optical data acquired by remote sensing. Due to its physical and chemical proprieties the atmosphere alters the spectral composition of photons reaching the sensor. To reduce the impact of variable atmospheric properties on the data, the two image mosaics were atmospherically corrected to apparent surface reflectance.

The Yosemite image mosaic was atmospherically calibrated using the program ACORN Mode 3 (Atmospheric Correction Now! (ACORN:Analytical Imaging & Geophysics). In order to use this program some field spectra of flat calibration targets were made using the full range (400-2500 nm) field spectrometer, Analytical Spectral

Device (ASD). Because the models incompletely correct for atmospheric scattering and absorptions (especially high uncertainty in the aerosol and smoke or particulate retrievals), we performed a standard secondary empirical correction. This method uses known reflectance of large plots of many pixels of "invarant" targets (ones that don't change with time and are spectrally homogeneous) that can be used to calibrate the imagery to the known reflectance. In particular light targets (sand) and black targets (asphalt) were considered good targets that were easily visible in the image. Using this process we obtained a very good calibration result, based on comparisons with field spectra.

The Kings Canyon image mosaic was atmospherically corrected using ACORN Mode 2. In this case only one target field spectra was used.

Georectification

The georectification was performed using as base map the USGS Digital Orthophoto Quarter Quadrangles (DOQQ). Since both study areas are mostly undeveloped, it was somewhat difficult to find good control points to register the images, so the actual final georectification of the images was not as precise as we prefer. Dr. Joe Boardman (AIG, Inc.) has been commissioned by USGS to develop an orthophoto correction algorithm and he appears to have tested this on data from Yosemite National Park. However, at this time we have not received a copy of this data to compare to our geocorrected data.

Vegetation classification

The classification of the forest vegetation in both the images was an important step of the analysis. In fact, since ozone damage is remotely detectable only on Jeffrey and Ponderosa Pine, a classification map that delineates their distribution within the forests would significantly improve the results. With an accurate land cover classification we could easily recognize the location of just these species and mask the rest of the image in order to show any spatial differences in physiology related to ozone exposure.

To test this, two different classification methodologies were applied to the images. For Yosemite National Park we used the Spectral Angle Map (SAM) supervised classification, while for Sequoia/Kings Canyon National Park the ISODATA unsupervised classification was applied. In the first case image spectra were selected and considered as potential endmembers for the analyses. The field campaigns and the vegetation class map in vector format, computed by the Cooperative National Park Studies Unit (University of California, Davis), allowed us to identify pure pixels of several different potential classes in some of the image. Then, considering the spectral signatures of these pure pixels we defined the spectral library (the set of potential endmembers) used for the SAM classification.

For Kings Canyon due to the scarce amount of field data and vegetation vector data, we could apply only an unsupervised classification, which actually did not allow recognition and classification of different coniferous species.

Advanced analysis

In order to detect the crown ozone injuries in yellow pines, the Normalized Difference Vegetation Index (NDVI) was calculated for both Yosemite and Kings Canyon images.

In details through the image classification it was possible to mask all the classes that were not believed to be yellow pines. NDVI was calculated just for these masked images. NDVI is a standard widely used vegetation index that is a ratio of reflectance in red and near-infrared bands. It is known to be highly correlated to leaf area although canopy architecture and presence of standing and dead litter cause some degredation of the results when applied to a heterogeneous scene.

Following this step, the crown water content was calculated for the yellow pine images. For this purpose the entire spectrum for all vegetated pixels were examined. In fact considering that water in the leaves absorbs strongly at wavelengths: 0.965, 1.4, 1.9 and 2.7 µm (water absorption bands), we analyzed the spectral absorption depth corresponding to the 0.965µm band.

Results

The sites

Table 1. Site characteristics

Site	Moisture Regime	Elevation (m)	LAI (m^2 m^{-2})† Total/Projected	Latitude/Longitude
Lower Yosemite	wet	1214	0.25/0.107	37.73ºN, 119.64ºW
Upper Yosemite	dry	1251	0.21/0.093	
Lower King's Canyon	wet	1527	0.33/0.143	36.80ºN, 118.58ºW
Upper King's Canyon	dry	1578	0.17/0.075	

† Leaf Area Index of pines within plot only, no other species are included

A significant difference in upper and lower sites was the length of sunlit day. Lower sites were within valleys with steep walls, thus days were shorter. During the time of the year when the sun was low – late fall to early spring – the lower King's Canyon site received little sun because of Sentinel Peak to the south. Several problems, including paucity of solar power, kept the lower King's Canyon site inoperable until the multiple problems were sorted out and fixed in November 2002.

Specific leaf areas, measured in August and September 2002, were significantly higher in Yosemite *Pinus ponderosa* than in King's Canyon *Pinus Jeffreyi*, but not significantly different between sites within park (two-tailed T-test, including 3 age cohorts, $P<0.05$). Upper Yosemite was the densest plot when all tree species were considered. That site included emergent incense cedar, black oak and Douglas-fir, and numerous understory trees.

Patterns in soil moisture, water potential and VPD

Soils at the Yosemite lower site were of the Miwok complex, extremely sandy loam, slopes 1-5%. At the upper site, soils were Half Dome, extremely stony sandy loam, 10-25% slopes (SCS 1994). Soils at King's Canyon sites were extremely sandy loam, upper site 10-25% slopes, lower site 0-5% slopes. Soils at all sites dried from May onward and reached minimum moisture at 50cm by the beginning of August. Soils were dry through the end of October. By the mid- November soils had resaturated in response to winter rains. Figure 6a. The lower sites were generally wetter than the upper sites, especially in the winter and spring. However, by mid-summer differences at the 50 cm depth had disappeared, or in the case of the King's Canyon sites, reversed (Figure 6b). Soil drought at 50 cm does not necessarily indicate that trees are water stressed, as ponderosa pine have been documented to reach deep water, well below the 0.5-1 m typically measured. Water potential measurements are a much better indicator of water stress.

Water potential measurements in both 2002 and 2003 showed a similar pattern. The pine were not drought-stressed in May at any of the sites. By mid-September, however, the upper Yosemite site was experiencing drought stress while the lower Yosemite site was not (Figure 7a,b). The lower King's Canyon site was not significantly different from the upper King's Canyon site in September – both were drought stressed. Trees appeared to be more drought-stressed in 2002 than in 2003, consistent with the greater rainfall in 2003.

Vapor pressure deficit (VPD) at all the sites was remarkably similar over the year and a half study period (Figure 8a). Unexpectedly, the lower site at King's Canyon had higher VPD in the growing season than the upper sites and the difference increased with increasing VPD (Figure 8b). In Yosemite, the sites were very similar. The difference at both locations was greater in 2003 than in 2002.

Seasonal patterns in transpiration and conductance

Yosemite

Mean mid-day transpiration (from 10:00 – 14:00 PST) in Yosemite reached a maximum in mid-July (JD 200), then declined thereafter, probably in response to decreasing soil water availability. The peak seen at the lower site was absent at the upper site. The pattern was consistent with higher water availability at the lower site during the growing season. Transpiration during the growing season was much greater at the lower Yosemite site than at the upper site (Figure 9a). During the winter months, transpiration was similar at both sites. Sap flow instruments failed at the end of August 2003 at the lower Yosemite site, so contrasts between sites is impossible after that time.

Mean mid-day stomatal conductance declined over the growing season, but increased once rains resaturated the soils in the fall. During the growing season, conductance was greater at the Yosemite lower site than at the upper site (Figure 9b, 10b,c).

King's Canyon

Sap flow instruments were non-functional at the lower King's Canyon site until November 2002, thus the only data on differences between sites during the growing season was in 2003. Mean mid-day transpiration in King's Canyon declined over the

growing season, probably in response to observed decreased soil water availability (Figure 11a). Transpiration was not different between sites, until early August when the lower site had lower values than the upper site. This could very likely be explained by the occlusion of sun late in the season by Sentinel Peak. Winter transpiration values were lower at the lower site than the upper site, probably for the same reason.

Mean mid-day stomatal conductance also declined over the growing season (Figure 11b). Conductance was very similar between upper and lower sites during the 2003 growing season (Figure 10a).

Seasonal patterns in ozone uptake

Differences in stomatal ozone uptake (defined as ozone concentration $\times$ stomatal conductance to ozone) were influenced by differences in both ozone concentration and conductance. In Yosemite, ozone concentration at the upper site was consistently 8.5 ppb higher than lower site ozone concentration, as observed with passive monitors (Figure 12, R^2=0.8, slope = 0.97, intercept=8.5). Upper site ozone concentration was also highly correlated with ozone concentration at the Turtleback Dome site (R^2=0.85, slope = 0.86, intercept = -6.0), which represents regional ozone concentration.   Yosemite Valley ozone concentration is very different than regional, as Valley air is influenced by local NO_x sources (Dillon and Panek, in progress). Finally, lower site passive ozone concentration more closely mirrored actively measured ozone concentration at the Merced River site (Figure 12). Thus, while the lower Yosemite ozone concentration was similar to Valley air, the upper Yosemite concentration was influenced by both regional and Valley ozone concentrations, and represents some mix of both. Thus, upper site ozone concentration was estimated as Merced River site ozone concentration + 8.5 ppb.

Mean mid-day ozone uptake was higher at the lower site at all times of the year, despite higher ozone concentrations at the upper site (Figure 13a). Ozone uptake was highest in spring despite low ozone concentrations at that time of year. And while ozone concentrations peaked in mid-summer, ozone uptake was not the highest at this time of year because of low conductance (Figure 13a).

Stomatal ozone uptake was similar at the King's Canyon lower and upper sites in the 2003 growing season because of similarities in stomatal conductance. At both sites, ozone uptake was at a maximum in the spring around late April/early May (Figure 13b, JD 120-150). Despite much higher ozone concentrations in the later growing season, ozone uptake progressively declined from May onward, reflecting stomatal constraint (Figure 13b). Passive ozone data showed no consistent difference between ozone concentration at Cedar Grove, where the active monitor was, and Road's End, where the instrumented trees were (data not shown). Thus, no adjustments were made for ozone concentration at the different sites, and any differences in ozone uptake would have been driven by differences in stomatal conductance.

Diurnal patterns in ozone uptake

In Yosemite, during the winter and late spring, the diurnal ozone uptake pattern was similar at the two sites. However, by late summer the diurnal pattern had diverged so that

ozone uptake was higher at the lower, mesic site than at the upper xeric site. Peak ozone uptake occurred in the early morning, around 8:00 PST during the summer, 4-5 hours before peak ozone concentrations (Figure 14a). In the winter, peak ozone uptake and ozone concentration occurred around noon (Figure 14a). Under mesic spring conditions, the diurnal trend at both sites was bimodal – that is there was a major peak in the early morning, and a smaller peak in the mid-afternoon, around 15:00 PST.

In King's Canyon, there were no differences between the upper and lower sites at any time of the year. As at the Yosemite sites, however, peak ozone uptake preceded peak ozone concentration by about 4-5 hours (Figure 14b) Peak ozone uptake occurred around 9:00 PST during the growing season, and around noon in the winter (Figure 14b). The trends at both King's Canyon sites were bimodal during the growing season.

Ozone uptake summaries

Although the seasonal designations typified by mesic climates are not natural seasonal breakpoints for the Mediterranean climate of California, those designations were used to divide the year for comparative purposes with other sites. Fall is designated as September 21 until December 21, winter until March 21, spring until June 21, and summer until September 21. By far the season of greatest ozone uptake was spring at all the sites, with as much as 2.5 times the uptake of the summer (Figure 15). Significant uptake occurred in the fall and winter. The Yosemite lower site had greater ozone uptake in the spring and summer than the upper site, but proportionally greater uptake during the drier season. During the fall and winter, the Yosemite sites were not very different. The King's Canyon sites were similar at all times of the year.

The site with the greatest annual ozone uptake was the lower Yosemite site, which was significantly greater than the upper site (Table 2). Both Yosemite sites had greater ozone uptake than the King's Canyon sites.

Table 2. Estimated ozone uptake in mol m^{-2} x 10^9.

	2002		2003		TOTAL
	Fall	Winter	Spring	Summer	
Lower Yosemite	4.96	4.66	16.13	8.80[†]	34.55
Upper Yosemite	3.23	3.89	13.76	5.08[†]	25.96
Lower King's Canyon	3.02	2.66	7.36	4.29	17.34
Upper King's Canyon	2.43	2.71	6.58	5.23	16.96

† Yosemite summer comparison is made from 2002 data, since the lower Yosemite site failed at the end of August 2003.

Within-site comparisons

To assess the potential for soil moisture to influence physiology *in situ*, particularly ozone uptake, within-site comparisons were made between a wet period (the last 2 weeks of June) and a dry period (the last 2 weeks of October). Ratios of dry to wet showed that all sites showed significant reductions over the growing season, except the lower

Yosemite site, which showed increases in physiological activity and consequently in ozone uptake. The reductions in stomatal conductance and ozone uptake were greatest at the King's Canyon site (Table 3). The effect of drought on the King's Canyon pine was to cause a reduction in ozone uptake of 80-90%. The effect of drought on upper Yosemite pine was a reduction in ozone uptake of around 50%.

Table 3. Ratios (dry/wet) of mean mid-day values, averaged over the last 2 weeks of June (wet) and the last 2 weeks of October (dry).

Site	Stomatal Conductance	Ozone Uptake
Lower Yosemite	1.35	1.60
Upper Yosemite	0.64	0.53
Lower King's Canyon	0.13	0.09
Upper King's Canyon	0.18	0.14

Physiology and parameters for modeling

At the leaf level, photosynthesis showed the least change from May to September (Figure 16a). While values at all sites peaked around 6-7 μmol m^{-2} s^{-1} in May, sites diverged in September. Peak values were higher at the wet, lower sites in September, although the trend was obscured by high within-site variation, especially at King's Canyon. The minor effect of drought on photosynthesis may be explained by changes in water-use efficiency, as detailed below.

In contrast to photosynthesis, drought had a profound seasonal effect on conductance at the leaf level at both sites (Figure 16b). The between season differences were greater than the between site differences. Again, while the wet lower sites exhibited higher conductance values than the dry upper sites in September, variation masked any significance to the differences between wet and dry sites.

Transpiration followed a similar pattern as conductance (Figure 16c). Drought had a significant seasonal effect at both sites. The lower sites had higher transpiration rates than the upper sites in September, however large variation obscured any significance differences between wet and dry sites.

Instantaneous water-use efficiency (WUE), measured as photosynthesis divided by stomatal conductance, or alternatively photosynthesis divided by transpiration normalized to VPD, increased significantly from May to September ($P<0.01$) at all the sites (Figure 17). This change is consistent with the fact that photosynthesis did not drop dramatically between May and September. It is also consistent with previous research which shows a similar increase in WUE in response to drought (Panek 2004, Panek and Goldstein 2001).

V_{cmax} and J_{max} showed slight, non-significant declines between May and September at all sites, except for the upper Yosemite site, where the difference was highly significant ($P=0.01$, Figure 18). Dark respiration (Rd) showed no change at any of the sites that was significant at the 0.05 level (Figure 18).

Quantum efficiency was not significantly different between sites (Table 3). Maximum photosynthesis was highest at the upper Yosemite site, significantly higher than the other site (P<0.05), while the lower King's Canyon site was the lowest. Light compensation point was significantly higher at the lower sites, where daylength was shorter, than at the upper sites (Table 4).

Table 4. Results from light curve analysis.

Site	Quantum Efficiency	P_{max}	Light Compensation Point
Lower Yosemite	0.018 a	5.3 a	42.1 b
Upper Yosemite	0.024 a	7.7 b	16.8 a
Lower King's Canyon	0.017 a	3.2 c	34.9 c
Upper King's Canyon	0.020 a	5.5 a	15.4 a

Different letters are significantly different at the 0.05 level.
Units: Quantum efficiency (mol CO_2 uptake quanta light^{-1}); P_{max} (μmol CO_2 m^{-2} s^{-1}); Light compensation point (μE m^{-2} s^{-1}).

Ozone injury

Ozone injury was slightly greater on trees at the lower sites than the upper sites (Table 4). This result was consistent with either measure of injury used, OII or chlorotic mottle alone. Ozone Injury Index (OII) is a function of visible injury, fascicle retention, foliar length and crown health (Miller et al. 1996), of which chlorotic mottle is a part. Using the suite of variables represented in OII, the site with the greatest injury was lower Yosemite. Differences in OII and chlorotic mottle between upper and lower sites were not significant at the 0.05 level. There was no mottle on current foliage at the Yosemite sites, and very little at the King's Canyon sites. Chlorotic mottle was progressively worse with increasing age class, as would be expected as the injury is cumulative.

Table 4. Results from branch injury analysis.

Site	OII[†]	Chlorotic Mottle			
		2000	2001	2002	2003
Lower Yosemite	48.5 ± 10.3	1.8	0.8	0.6	0
Upper Yosemite	43.1 ± 3.1	1.3	0.8	0.5	0
Lower King's Canyon	45.7 ± 14.7	2.5	1.7	0.7	0.4
Upper King's Canyon	39.2 ± 15.0	1.8	1.0	0.8	0.3

† OII is a function of visible injury, fascicle retention, foliar length and crown health.

Modeling

STOMATA, described above, was run at the Yosemite upper and lower sites using measured site meteorological data and physiological parameters V_{cmax} and J_{max}. The

model fit was good for the upper site (R^2=0.51, Figure 19a). However, the model fit was poor for the lower site (R^2=0.36, Figure 19b) because of model sensitivity to soil moisture. Soil moisture measurements at the lower site did not accurately measure the soil water which the trees had access to below 50 cm. Since the trees had access to more moisture than was measured, soil moisture was doubled in the model after moisture had dropped below 0.8 MPa, at around JD 160. The increase in soil moisture greatly improved the fit of the model (R^2=0.52, Figure 19b).

The model did a good job of capturing seasonal variation in stomatal conductance in both years and at both sites (Figures 20, 23). The progressive decline in stomatal conductance was captured, and the increase once rains began in the fall.

The diurnal variation was captured with the model, at both sites. The early morning stomatal opening, the quick peak in conductance, and the bimodal nature of the measured diurnal curve were well represented by the model (Figures 24 a, b).

Remote sensing results

The results of mapping the NDVI across the masked imagery obtained a map that was positively correlated to chlorophyll content and inversely to ozone damage. From this analysis, we show that the study areas where field data were taken in the Upper Yosemite has a higher NDVI value with respect to the Lower Yosemite. A different pattern emerges for leaf water content for which little difference was found between the Upper and Lower Yosemite areas. However considering the distribution of the pixels in the NDVI image (Figure 21) it appears that there is a correlation between the topographic location of the trees and the pixel NDVI value (Figures 4 and 21). We obtained the same pattern of results for the Kings Canyon study area. Moreover when combing the NDVI with the water content values we observe a decrease in NDVI values (increased of chlorosis) with decreased water content (Figure 22). This is consistent with lower leaf area (since chlorophyll and water are highly correlated being co-located in the leaf) as would occur in low density vegetation for a variety of reasons, possibly unrelated to ozone exposure (Figure 22). At least some of this confusion is due to problems with calibration (e.g., albedo differences on sunlight and shady side of the valleys) and georegistration. The main problem appears to be that for most of the vegetation at the site, there is no effect (or a minor effect) due to ozone exposure and because of the natural heterogeneity, there is no pattern between water content and ozone exposure. Alternatively the width of the data cloud shown in the scatterplot may be related to sites with more or less exposure to ozone since a large number of pixels cover the full range of NDVI at constant water content values. Pixels on the right side of the data cloud (i.e., high NDVI side) and have low water content (near the x-axis) are candidates for ozone damage combined with water stress. The patterns we observe are suggestive that if the data is stratified by land cover type, to identify the ozone sensitive species, we may still show a spatial pattern related to ozone exposure. We are continuing to pursue these results to test this hypothesis.

Discussion

Patterns in environmental variables

Summer drought and winter resaturation occurred as expected. Soil moisture dropped and VPD increased over both growing seasons 2002 and 2003. Winters were wet, but only moderately cold. Soil temperatures never dropped below freezing (data not shown).

While soil moisture is the primary determinant of physiological response, soil moisture measured at 50 cm did not reflect the drought experienced by trees, as seen in water potential measurements. Water potential data showed that, while all trees were unstressed by drought in May, by September the upper Yosemite site trees were very stressed and the lower Yosemite trees were not. However, the soil moisture data from September showed minimum soil moisture at both upper and lower Yosemite sites. Thus, the lower Yosemite site trees were getting their water from depths lower than 50 cm. It has been well-documented that yellow pine can tap into water sources at great depth, and sometimes as far as 9 m away from the tree.

Data showed that proximity to year-round water was not a good surrogate for soil moisture. Both the "wet lower" and "dry upper" King's Canyon sites were very similar in drought regime – both were drought-stressed, even though the lower site was within what appeared to be a flood plain, near the height of the water table, and within 100 feet of the King's River. Thus the comparison between mesic and dry sites is only valid in Yosemite, while King's Canyon serves as 2 more examples of late-season dry sites.

Patterns in physiological variables

Whole tree level

All sites experienced a progressive decrease in transpiration, conductance and ozone uptake over the growing season in response to drying soils and decreasing atmospheric humidity. However, as hypothesized, the decrease was greater in the upper dryslope site (and the King's Canyon sites) than in the lower riparian site. The mesic site maintained greater physiological activity through the summer drought.

In the winter and spring, when soils were saturated and VPD was low, the difference between physiology of dry and wet site disappeared. During the growing season, there was very little scatter in the physiological data, because the factor controlling physiology – soil moisture – showed very little day-to-day variability.   In the winter, however, all sites exhibited high variation in physiological variables, because controlling variables at that time – temperature and light – were highly variable in the winter.

The highest conductance values were in the late spring at all sites, when temperature, soil moisture, and radiation were highest concurrently. Ozone uptake was highest at that time, even though ozone concentrations were not the highest of the year. Consistent with previous leaf-level studies, ozone concentrations peaked in August at both locations, but by then stomatal limitation was great, thus ozone uptake was low. Unlike other climate zones in the United States, winter ozone uptake occurred, due to typical mild Sierra Nevada winters. Soil temperatures never dropped below 0ºC, so trees remained active all winter. Frequent excursions of air temperature to 15-20ºC in January-February 2003

meant that trees had ideal conditions for photosynthesis, conductance and thus ozone uptake, even though it was winter.

Within-site effects of water availability were profound. At the Yosemite dry upslope site, ozone uptake decreased by 50% between June and October due to drought stress. At the King's Canyon site, the effect was even greater. Ozone uptake declined by 80-90% between June and October due to drought stress. It cannot be assumed that the availability of water late in the season would cause such a profound effect, but it suggests that had the King's Canyon trees had access to water in October, there would have been significant summer ozone uptake.

Between-site effects of water availability were great. As hypothesized, the site with the greatest annual ozone uptake was the site with greatest year-round access to water – the mesic, lower Yosemite site. Annual ozone uptake at the lower site was 33% greater than the upper site. Even though uptake was similar in the winter between the upper and lower Yosemite sites, differences in the growing season made up for lack of differences in the wet season. Both Yosemite sites had greater ozone uptake than the King's Canyon sites.

Diurnal patterns of ozone uptake show that peak ozone uptake preceded peak ozone concentration by 4-5 hours, at all the sites in the summer months. In the summer, ozone uptake peaked sharply with conductance in the early morning hours. Uptake then tapered to a shoulder or a secondary peak later in the day, and then stopped with stomatal closure at sunset. In the late summer, daily peak ozone uptake at the mesic, lower Yosemite site was 46% higher than uptake at the dry upper site.

Leaf level

At the leaf level, physiological patterns in response to seasonal drought were similar. Conductance and transpiration dropped in response to summer drought stress. Differences between sites were not as evident at the leaf level as at the whole tree level, probably due to at least 2 factors. First, one low branch does not represent the entire tree in the same way sap velocity measurements do. Second, trees with branches close to the ground were spread out further and were not uniform in size, leading to greater variation in the measured variable. For example, one large tree at the lower King's Canyon site was within 10 feet of the water, and had roughly 2-3 times the physiological response as the other measured trees in September, leading to great variability at that site.

Photosynthesis showed the least decline in response to summer drought at any of the sites. This was in large part due to changes in water-use efficiency, which increased at all sites, regardless of whether the site was drought-stressed. The site which showed the most significant decline in photosynthesis over the season was the upper Yosemite site. V_{cmax} and J_{max} declined here in response to drought stress and not at the lower Yosemite site. Respiratory carbon losses decreased in response to decreasing soil moisture. Overall, photosynthetic activity decreased at the upper Yosemite site in relation to the lower site. Response to light (Table 4) showed that both lower sites had significantly greater light compensation points than upper sites. This difference, perhaps because of the lower annual radiation due to steep valley sides occluding the sun, also confounded any difference in photosynthesis due to drought stress alone.

Ozone Injury

The pattern of ozone injury suggests that drought stress and ozone uptake are important, but that the true relationship between injury and uptake may be more complex than this study was able to explain. The focus of this study was not on injury, thus these results should be considered preliminary and the basis for further exploration. Lower Yosemite trees showed more injury than upper Yosemite trees, as would be expected if ozone uptake were directly related to injury. However, the relationship was not significant at the 0.05 level, using either the suite of variables represented in OII, or chlorotic mottle alone. To truly elucidate the relationship between injury and uptake would require re-sampling with an increased sample size.

Modeling

STOMATA is very sensitive to soil moisture. With the inaccurate measurement of available soil moisture at the lower Yosemite site, the model was unable to predict the stomatal behavior of the pine. However, when the soil moisture was corrected to a representative value, the model predicted stomatal behavior adequately at the lower site. At the upper site, the model predicted physiological response adequately without modification. The model predicted the seasonal variability in conductance with reasonable accuracy at both sites. It captured the drop in conductance over the growing season and the sudden rise with November rains. The model also captured diurnal variation, including early morning stomatal opening, the sharp peak in early morning conductance, and the afternoon sub-peak of the measured diurnal curve. Although STOMATA was designed for leaf-level conductance prediction, it did well at the stand level, thus appeared to scale well. This is very likely in part a result of the open nature of the pine canopy. The model is thus a good tool for estimating canopy conductance, and thus ozone uptake, at sites throughout the Sierra Nevada.

One limitation to the application of this model is the difficulty of accurate measurement of relevant soil moisture. Soil moisture at 50 cm was not a good predictor of water stress in pine at the lower riparian Yosemite site, although it was at the upper dryslope site. How to estimate water stress in trees with access to water well below the measurable depth can only be done with canopy water stress measurement (direct or remotely sensed) and modeling. As this study showed, distance to water was not necessarily a good predictor of availability of water in a riparian zone, as the lower King's Canyon trees didn't have access to water from the nearby King's River.

Remote Sensing Techniques

The use of remote sensing techniques to assess water stress of the canopy is a necessary component of accurately modeling canopy conductance, and thus ozone uptake, at the landscape scale. The tools developed by Ustin et al. (1999, 1998) have been applied to the remotely sensed images of Yosemite Valley and King's Canyon, taken by NASA at peak drought stress in October 2002. Details are reported here.

Conclusions

The heterogeneous distribution of water across the landscape has a profound effect on pine forest physiology, as hypothesized. Pine with year-round access to water had higher stomatal conductance during drought periods and took up 33% more ozone annually than trees that experienced growing season drought stress. Furthermore, temporal changes in water availability *in situ* caused dramatic physiological response and consequent changes in ozone uptake, which were site-dependent. The most dramatic decrease in ozone uptake over the growing season was at King's Canyon, where ozone uptake was limited 80-90% by drought stress.

Studies such as this one can serve as proxies of expected impacts due to climate change. The results reported here suggest that changes in timing and amount of snowmelt which are anticipated with predicted changes in climate, will profoundly influence pine physiology, including ozone uptake. Current forecasts of climate change in the California Sierra Nevada indicate that both temperature and precipitation will increase. Most precipitation is forecast to fall in the winter and spring months, however, and variability in the timing and duration of rain events is expected to increase. Increased temperatures are predicted to diminish the snowpack and, despite the increased precipitation, may lead to drier summers. Thus, the period of physiological dormancy will lengthen in pine forests, protecting them from ozone uptake, but also limiting carbon uptake. The distribution of water across the landscape can be expected to play a greater role in forest health.

Acknowledgements

References

Arbaugh, M. J., P. R. Miller, J. J. Carroll, B. Takemoto, and T. Proctor. 1998. Relationships of ozone exposure to pine injury in the Sierra Nevada and San Bernardino Mountains of California, USA. *Environmental Pollution*, 101, 291-301.

Asner, G. P. 1998. Biophysical and biochemical sources of variability in canopy reflectance. *Remote Sensing of Environment*, 64, 234-253.

Asner, G. P., C. A. Wessman, and C. A. Bateson. 1998a. Sources of Variability in Plant Canopy Hyperspectral Data in a Savanna Ecosystem., Cooperative Institute for Research in Environmental Sciences,, Boulder, CO.

Asner, G. P., C. A. Wessman, and D. S. Schimel. 1998b. Heterogeneity of savanna canopy structure and function from imaging spectrometry and inverse modeling. *Ecological Applications*, 8, 1022-1036.

Baldocchi, D., B. Hicks, and T. Meyers. 1988. Measuring biosphere-atmosphere exchanges of biologically related gases with micrometeorological methods,. *Ecology*, 69, 1331.

Baldocchi, D. D. 1989. Turbulent transfer in a deciduous forest. *Tree Physiology*, 5, 357-377.

Baldocchi, D. D. 1997. Measuring and modeling carbon dioxide and water vapor exchange over a temperate broad-leaved forest during the 1995 summer drought. *Plant, Cell and Environment*, 20, 1108-1122.

Ball, J. T., E. Woodrow, and J. A. Berry. 1987. A model predicting stomatal conductance and its contribution to the control of photosynthesis under different environmental conditions. *In* Progress in Photosynthesis Research, J. Biggins, ed., M. Nijhoff Publishers, Dordrecht, 221-224pp.

Bauer, M. R., A. H. Goldstein, J. A. Panek, and N. E. Hultman. 2000. Ozone deposition to a ponderosa pine plantation in the Sierra Nevada Mountains (CA): a comparison of two different climatic years. *J. Geophysical Research - Atmospheres*, 105(D17), 22123-22136.

Becker, P., and W. R. N. Edwards. 1999. Corrected heat capacity of wood for sap flow calculations. *Tree Physiology*, 19(11), 767-768.

Burgess, S. S. O., M. A. Adams, N. C. Turner, C. R. Beverly, C. K. Ong, A. A. H. Khan, and T. M. Bleby. 2001. An improved heat pulse method to measure low and reverse rates of sap flow in woody plants. *Tree Physiology*, 21, 589-598.

Bytnerowicz, A. 1996. Physiological aspects of air pollution stress in forests. *Phyton (Horn)*, 36(4), 15-22.

CARB. 1999. Historical statewide emissions and air quality. Air Resources Board 1999 Almanac, C. A. R. Board, ed., http://www.arb.ca.gov/aqd/ozone/ozgeosel.htm.

Clearwater, M. J., F. C. Meinzer, J. L. Andrade, G. Goldstein, and N. M. Holbrook. 1999. Potential errors in measurement of nonuniform sap flow using heat dissipation probes. *Tree Physiology*, 19(10), 681-687.

Darrall, N. M. 1989. The effect of air pollutants on physiological processes in plants. *Plant, Cell and Environment*, 12, 1-30.

Demerjian, K. L., U. K. Roychowdhury, S. Jin, and T. R. Lanni. 1992. Measurements of trace chemical constituents at Whiteface Mountain, Atmospheric Sciences Research Center, Albany, NY. 25-34.

Duriscoe, D. 1987a. Evaluation of ozone injury to ponderosa and Jeffrey pines in Yosemite National Park; 1985 Survey Results. *NPS/AQD Assignment 6, Contract CX-0001-4-0058*, Air Quality Division, NPS, USDI, Denver, CO. 68.

Duriscoe, D. 1987b. Evaluation of ozone injury to selected tree species in Sequoia and Kings Canyon National Parks; 1985 Survey Results. *NPS/AQD Assignment 6, Contract CX-0001-4-0058*, Air Quality Division, NPS, USDI, Denver, CO. 68.

Duriscoe, D. 1990. Cruise Survey of Oxidant Air Pollution Injury to Pinus ponderosa and Pinus jeffreyi in Saguaro National Monument , Yosemite National Park, and Sequoia and Kings Canyon National Parks. *NPS/AQD-90/003*, Air Quality Division, NPS, USDI, Denver CO 80225, Denver, CO. 1-.

Duriscoe, D. M., and K. W. Stolte. 1989. Photochemical oxidant injury to ponderosa (*Pinus ponderosa* Dougl . ex Laws) and Jeffrey pine (*Pinus jeffreyi* Grev . and Balf .) in the National Parks of the Sierra Nevada of California. *In* Effects of air pollution on western forests., R. K. Olson and A. S. Lefohn, eds., Air and Waste Management Association, Pittsburgh, PA, 261–278pp.

Field, C. B., G. C. Daily, F. W. Davis, S. Gaines, P. A. Matson, J. Melack, and N. L. Miller. 1999. Confronting Climate Change in California: Ecological Impacts on the Golden State. , Union of Concerned Scientists and Ecological Society of America, Cambridge, MA , Washington, DC. 62.

Gamon, J. A., H.-L. Qiu, D. A. Roberts, S. L. Ustin, D. A. Fuentes, A. Rahman, D. Sims, and C. Stylinski. 1999. Water expressions from hyperspectral reflectance: implications for ecosystem flux modeling. *In* Proceedings of the Eight Earth Science Airborne Workshop, Pasadena, CA, pp.

Gates, D. M. 1968. Transpiration and leaf temperature. *Annual Review of Plant Physiology*, 19, 211-239.

Granier, A., and D. Loustau. 1994. Measuring and Modelling the - Transpiration of a Maritime Pine Canopy From Sap-Flow Data. *Agricultural and Forest Meteorology*, 71(1-2), 61-81.

Green, R. O., D. Roberts, and S. Ustin. 1998. Mapping Agricultural Crops with AVIRIS Spectra in Washington State. *In* Seventh Earth Science Airborne Workshop,, Jet Propulsion Laboratory, Pasadena, CA,, pp.

Grulke, N. 1998. Physiological responses of ponderosa pine to gradients of environmental stressors. *In* Oxidant air pollution inpacts in the montane forests of southern California, P. R. Miller and J. R. McBride, eds., Springer, New York, 126-163pp.

Hatton, T. J., S. J. Moore, and P. H. Reece. 1995. Estimating stand transpiration in a *Eucalyptus populnea* woodland with the heat pulse method: measurement errors and sampling strategies. *Tree Physiology*, 15, 219-227.

IPCC, 1996. *Climate change 1995 : impacts, adaptations, and mitigation of climate change: scientific-technical analyses : contribution of working group II to the second assessment report of the Intergovernmental Panel on Climate Change*, Cambridge University Press, New York, NY. Pagespp.

Kurpius, M. R., M. McKay, and A. H. Goldstein. 2002. Annual ozone deposition to a Sierra Nevada ponderosa pine plantation. Atmospheric Environment **36**:4503-4515.

Lamanna, M. S., and A. H. Goldstein. 1999. In-situ measurements of C2-C10 VOCs above a Sierra Nevada ponderosa pine plantation. *Journal of Geophysical Research*, 104(D17), 21247-21262.

Leuning, R. 1995. A critical appraisal of a combined stomatal-photosynthesis model for C3 plants. *Plant, Cell and Environment*, 18(4), 339-356.

Marenco, A., H. Gouget, P. Nedelec, and J.-P. Pages. 1994. Evidence of a long-term increase in tropospheric ozone from Pic du Midi data series: consequences: positive radiative forcing. *Journal of Geophysical Research*, 99, 16617-16632.

Marshall, J. D., and R. H. Waring. 1986. Comparison of methods of estimating leaf-area index in old-growth Douglas-fir. *Ecology*, 67, 975-979.

Matyssek, R., W. M. Havranek, G. Weiser, and J. L. Innes. 1997. Ozone and forest in Austria and Switzerland. *In* Forest Decline and Ozone, H. Sandermann, A. R. Wellburn, and R. L. Heath, eds., Springer-Verlag, Berlin Heidelberg, 95-134pp.

McNaughton, K. G., and P. G. Jarvis. 1983. Predicting effects of vegetation changes of transpiration and evaporation. Water Deficits and Plant Growth, T. T. Kozlowski, ed., Academic Press, New York, 1-47.

Miller, P. R., R. Guthrey, S. Schilling, and J. Carroll. 1996. Ozone injury responses of ponderosa and Jeffrey pine in the Sierra Nevada and San Bernardino Mountains in California. *In* International Symposium on Air Pollution and Climate Change Effects on Forest Ecosystems, Riverside, CA. A. Bytnerowicz, M. J. Arbaugh, and S. Schilling, eds., pp.

Miller, P. R., J. R. Parameter, Jr., O. C. Taylor, and E. A. Cardiff. 1963. Ozone injury in the foliage of *Pinus ponderosa. Phytopathology*, 52, 1072-1076.

Misson, L., J. Panek, and A. H. Goldstein. 2004. A comparison of three approaches to modeling leaf gas exchange in annually drought-stressed ponderosa pine forests. Tree Physiology **24**:529–541.

Moncrieff, J. B., Y. Malhi, and R. Leuning. 1996. The propagation of errors in long-term measurements of land-atmosphere fluxes of carbon and water. *Global Change Biology*, 2, 231.

Monteith, J. L., and M. H. Unsworth. 1990. *Principles of Environmental Physics*, Edward Arnold, London. Pagespp.

National Park Service, U. 1999. Natural Resource Year in Review--1999. , A. Q. Division, ed., www.aqd.nps.gov/pubs/yir/yir99/pages/02challenges/challenges_briefs.htm.

Nikolov, N. T. 1997a. *Mathematical Modeling of Seasonal Biogeophysical Interactions in Forest Ecosystems*, dissertation, Colorado State University, Fort Collins.

Nikolov, N. T. 1997b. Modeling spatial distribution of leaf area index, canopy conductance to ozone, and fluxes of CO2, O3, and latent heat at the San Joaquin Valley (CA). , USDA FS, Fort Collins, CO. .

Nikolov, N. T., W. J. Massman, and A. W. Schoettle. 1995. Coupling biochemical and biophysical processes at the leaf level: an equilibrium photosynthesis model for leaves of C3 plants. *Ecological Modeling*, 80, 205-235.

Oren, R., N. Phillips, G. Katul, B. E. Ewers, and D. E. Pataki. 1998. Scaling xylem sap flux and soil water balance and calculating variance: a method for partitioning water flux in forests. *Ann. Sci. For.*, 55, 191-216.

Panek, J.A., D. D. Baldocchi, A. H. Goldstein. 2003. The need for spatially and functionally integrated models of ozone deposition to Sierra Nevada forests. Chapter for Elsevier book: Ozone Air Pollution in the Sierra Nevada – Distribution and Effects on Forests. Editors: *Andrzej Bytnerowicz, Michael Arbaugh, and Rocio Alonso.* Elsevier, Oxford. 388 pp.

Panek, J. A., M. Bauer, and A. H. Goldstein. 2002. An evaluation of ozone exposure metrics for a ponderosa pine ecosystem. Environmental Pollution 117:93-100.

Panek, J. A., and A. H. Goldstein. 2001. Response of stomatal conductance to drought in ponderosa pine: implications for carbon and ozone uptake. *Tree Physiology*, 21, 335-342.

Patterson, M. T., and P. R. Rundel. 1990. Ozone impacts on the photosynthetic capacity of Jeffrey pine in Sequoia National Park. *NPS/AQD–90/005*, Air Quality Division, USDI National Park Service, Denver, CO. 19.

Phillips, N., and R. Oren. 1998. A comparison of daily representations of canopy conductance based on two conditional time-averaging methods and the dependence of daily conductance on environmental factors. *Ann. Sci. For.*, 55, 217-235.

Pronos, J., and D. R. Vogler. 1981. Assessment of ozone injury to pines in the Southern Sierra Nevada, 1979/1980. *81-20*, USDA Forest Service, PSW. .

Reich, P. B. 1987. Quantifying plant responses to ozone: a unifying theory. *Tree Physiology*, 3, 63-91.

Rennenberg, H., A. Polle, and M. Reuther. 1997. Role of ozone in forest decline on Wank Mountain (Alps). *In* Forest Decline and Ozone, H. Sandermann, A. R. Wellburn, and R. L. Heath, eds., Springer-Verlag, Berlin Heidelberg, 135-162pp.

Roberts, D., K. Brown, R. Green, S. Ustin, and T. Hinckley. 1998. Investigating the Relationship Between Liquid Water and Leaf Area in Clonal Populus. *In* Seventh Earth Science Airborne Workshop, Jet Propulsion Laboratory, Pasadena, CA, pp.

Roberts, D., S. Ustin, S. Ogunjemiyo, Chen J., and T. Hinckley. 2001. Scaling up the Forests of the Pacific Northwest using Remote Sensing. *Ecosystems*, Submitted.

Roberts, D. A., M. O. Smith, and J. B. Adams. 1993. Green vegetation, nonphotosynthetic vegetation, and soils in AVIRIS data. *Remote Sensing of Environment*, 44, 255-26.

Runeckles, V. C. 1992. Uptake of ozone by vegetation. *In* Surface Level Ozone Exposures and their Effects on Vegetation, A. S. Lefohn, ed., Lewis Publishers, Inc., Chelsea, MI, 157-188pp.

Running, S., and J. Coughlan. 1988. A general model of forest ecosystem processes for regional applications. *Ecological Modeling*, 42, 125-154.

Sanderson, E. W., M. Zhang, S. L. Ustin, and E. Rejmankova. 1998. Geostatistical scaling of canopy water content in a California salt marsh. *Landscape Ecology 1*, 13, 79-92.

Serrano, L., S. L. Ustin, D. A. Roberts, J. A. Gamon, and J. Penuelas. 2000. Deriving water content of chaparral vegetation from AVIRIS data. *Remote Sensing of Environment*, 74(N3), 570-581.

Shuttleworth, W. J., J. H. Gash, C. R. Lloyd, C. J. Moore, J. Roberts, A. O. M. Filho, G. Fisch, V. P. S. Filho, M. N. G. Ribeiro, L. C. B. Molion, L. D. A. Sa, J. C. A. Nobre, O. M. R. Cabral, S. R. Patel, and J. C. De Moraes. 1984. Eddy Correlation Measurements of Energy Partition for Amazonian Forest. *Quarterly Jouranl of the Royal Meteorological Society*, 110, 1143-1162.

Skelly, J. M., A. H. Chappelka, J. A. Laurence, and T. S. Fredericksen. 1997. Ozone and its known and potential effects on forests in eastern United States. *In* Forest Decline and Ozone, H. Sandermann, A. R. Wellburn, and R. L. Heath, eds., Springer-Verlag, Berlin Heidelberg, 70-93pp.

Soil Conservation Survey. 1994. Soil Survey, Yosemite National Park. Yosemite Valley Part. In cooperation with USDI-NPS.

Stockwell, W. R., G. Kramm, H.-E. Scheel, V. A. Mohnen, and W. Seiler. 1997. Ozone formation, destruction and exposure in Europe and the United States. *In* Forest Decline and Ozone: A Comparison of COntrolled Chamber and Field Experiments, H. Sandermann, A. R. WEllburn, and R. L. Heath, eds., Springer-Verlag, Berlin Heidelberg, 1-38pp.

Stylinsky, C. D., W. C. Oechel, J. A. Gamon, D. T. Tissue, F. Migietta, A. Raschi, and S. Ustin. 2000. Effects of lifelong (CO2) enrichment on carboxylation and light utilization of *Quercus pubescens* Willd. examined with gas exchange, biochemistry and optical techniques. *Plant, Cell, and Environment*, 23(12), 1353 - 1362.

Teixeira Filho, J., C. Damesin, S. Rambal, and R. Joffre. 1998. Retrieving leaf conductances from sap flows in a mixed Mediterranean woodland: a scaling exercise. *Annales Des Sciences Forestieres*, 55(1-2), 173-190.

Treshow, M. E. 1984. Establishment of white pine biomonitoring plots in Acadia National Park. Final Report to US NPS, Air Quality Division, Lakewood. , US National Park Service. .

Ustin, S. L., D. A. Roberts, and Q. J. Hart. 1999. Seasonal Vegetation Patterns in a California Coastal Savanna Derived from Advanced Visible/Infrared Imaging Spectrometer (AVIRIS) Data. *In* Remote Sensing Change Detection: Environmental Monitoring Applications and Methods, C. D. Elvidge and R. Lunetta, eds., Ann Arbor Press, Ann Arbor, MI, 163-180 + color plate.pp.

Ustin, S. L., D. A. Roberts, S. Jacquemoud, J. Pinzon, M. Gardner, G. Scheer, C. M. Castaneda, and A. Palacios. 1998. Estimating canopy water content of chaparral shrubs using optical methods. *Remote Sensing of Environment*, 65, 280-291.

Zarco-Tejada, P. J., and S. L. Ustin. 2001. Modeling Canopy Water Content for Carbon Estimates from MODIS data at Land EOS Validation Sites. IGARSS Meeting, Sydney, Australia, pp.

Zhang, M., S. L. Ustin, E. Rejmankova, and E. W. Sanderson. 1996. Remote sensing of salt marshes: Potential for monitoring. *Ecological Applications*, 7(3), 1039-1053.

Figures
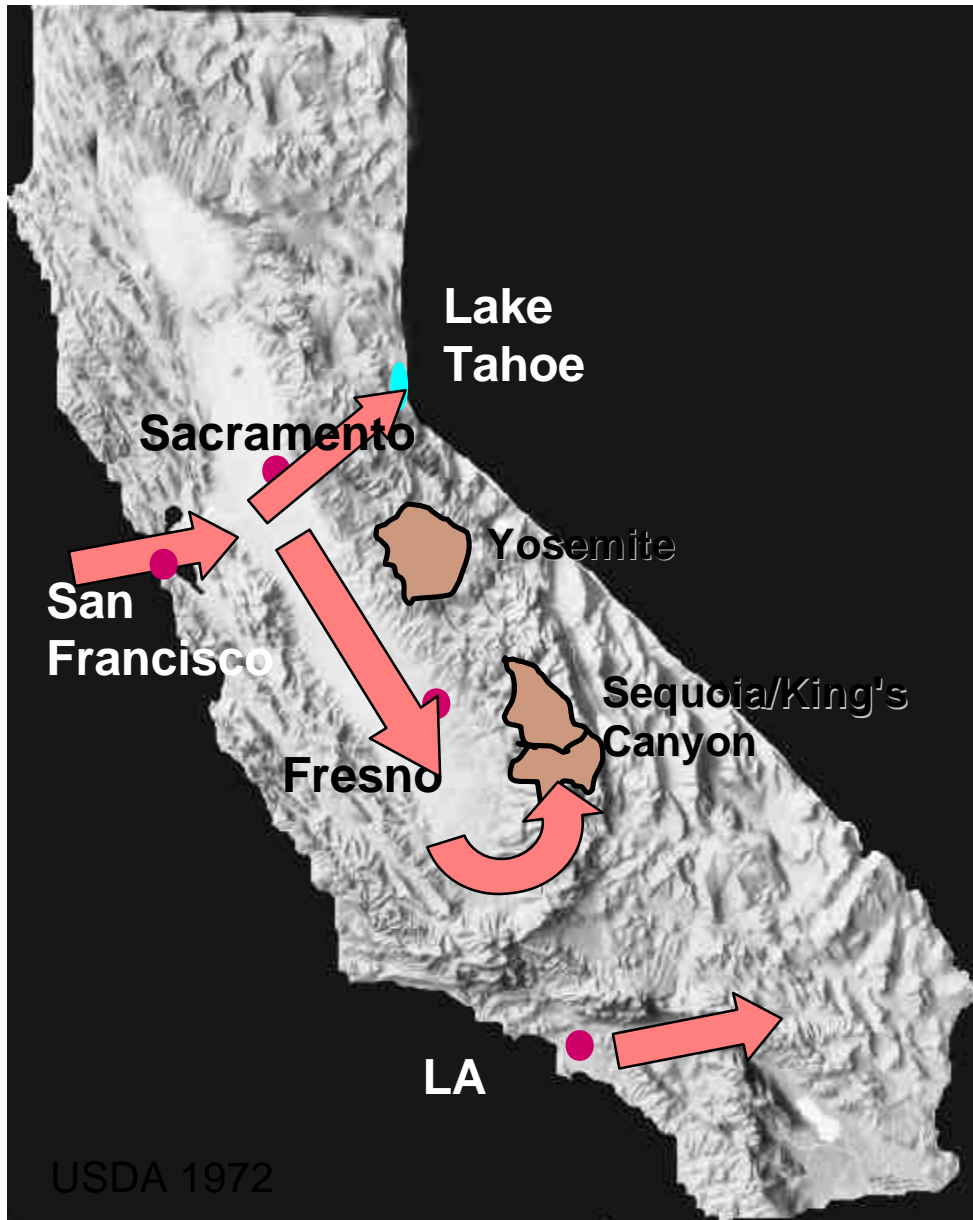
Figure 1. Air mass trajectories in California, shown in red, carry ozone and its precursors from source areas (cities, industrial areas and transit corridors) southwest until they are deflected up in to the forests of the Sierra Nevada by the transverse Tehachapi range. Thus, Sequoia Kings Canyon National Park is still one of the nation's most ozone-polluted parks, despite a general decrease in urban ozone concentrations over the last 20 years.
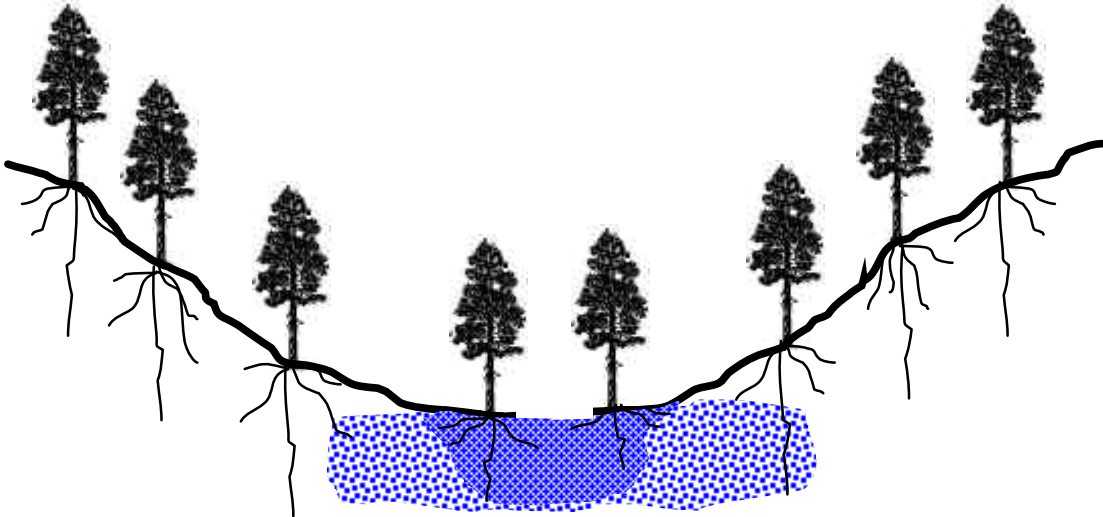
Figure 2. Sites were chosen to take advantage of a natural soil moisture gradient from sites with continuous availability of water through the California summer drought (riparian zone trees) to sites which are seasonally drought-stressed (dry upslope trees). One site is in Yosemite Valley (upper panel). The other site is similar, in King's Canyon.
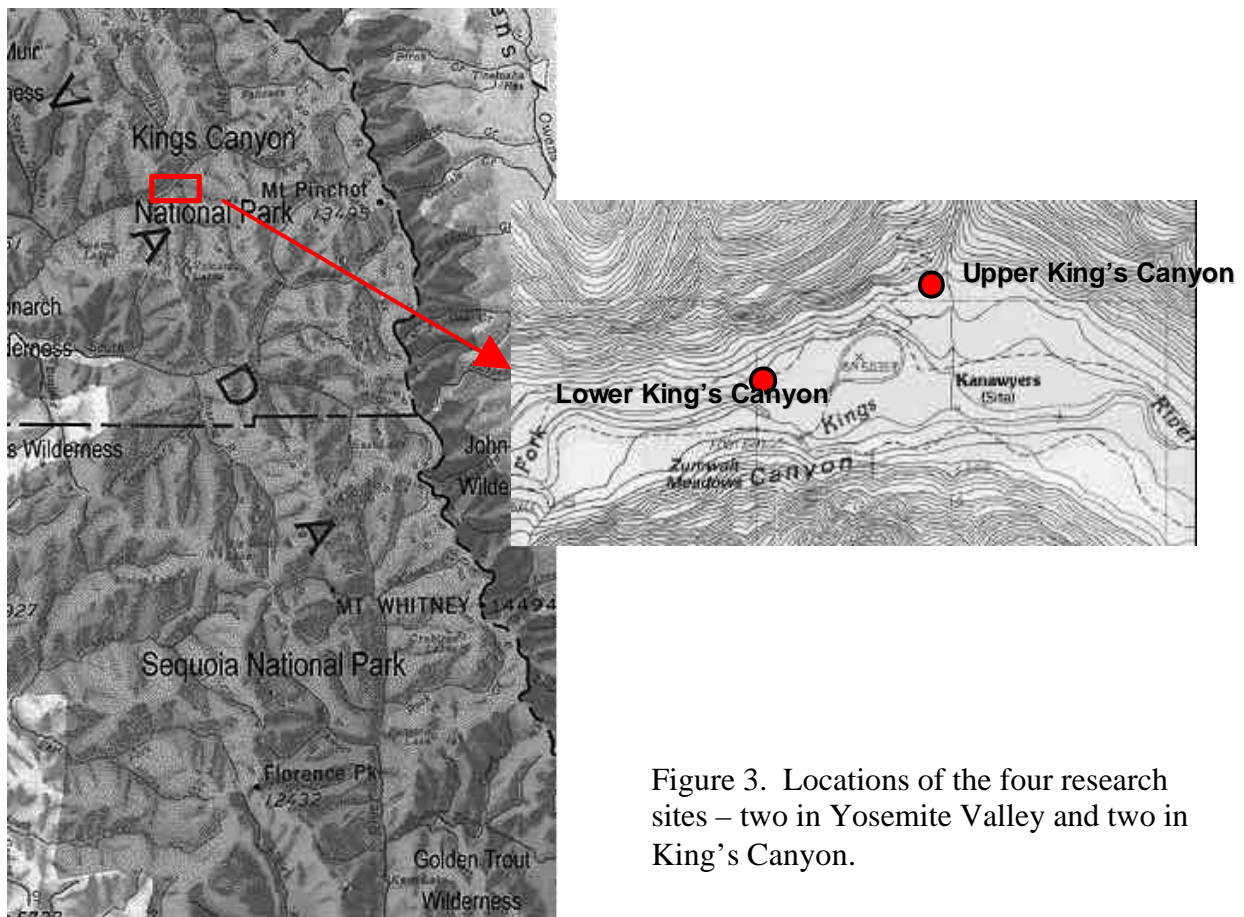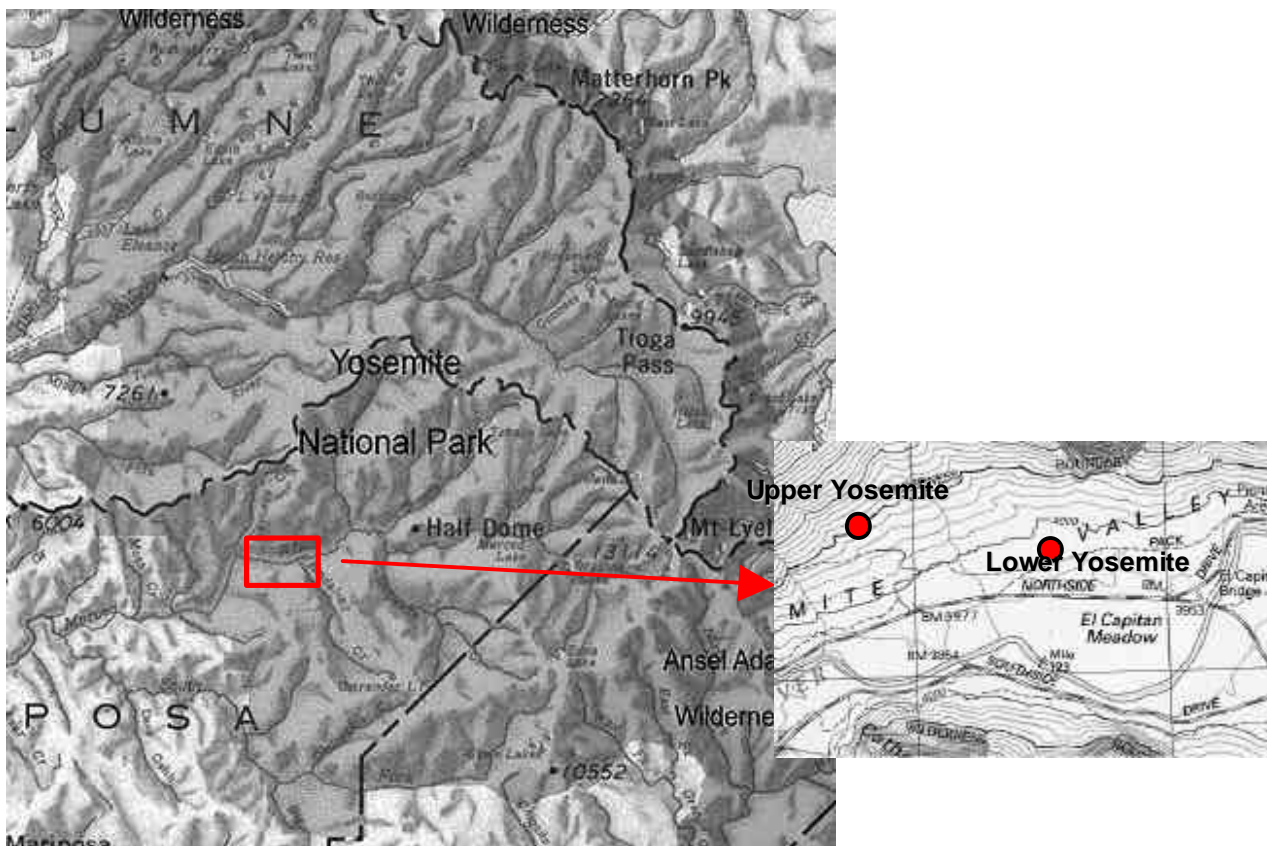
Figure 3. Locations of the four research sites – two in Yosemite Valley and two in King's Canyon.

Figure 4: Yosemite Valley map with the overlapping of the AVIRIS flight line used for the project.
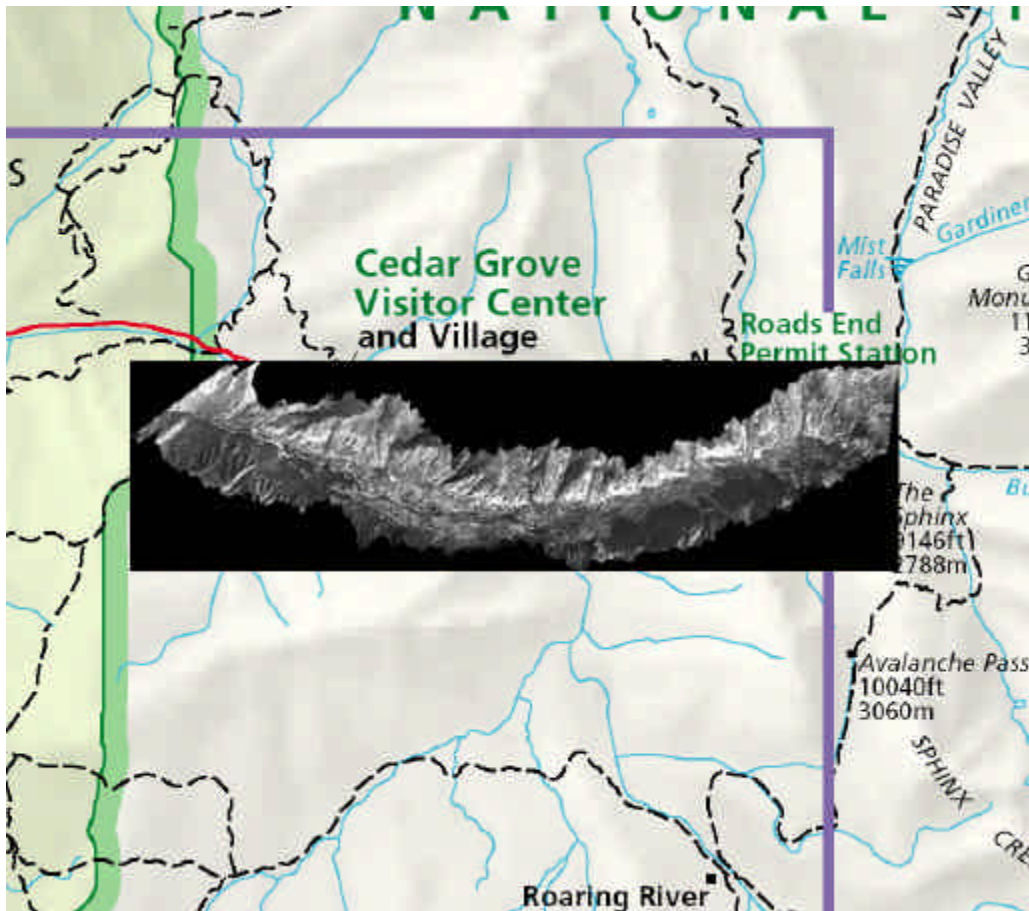
Figure 5: Kings Canyon National Park map with the overlapping of the AVIRIS flight line used for the project.
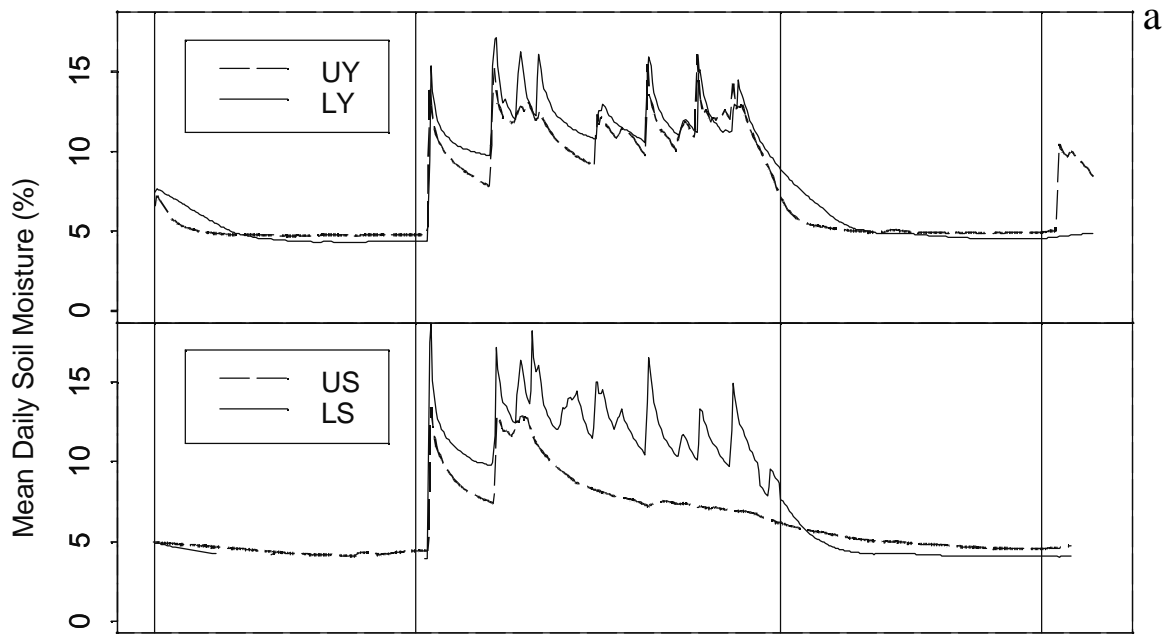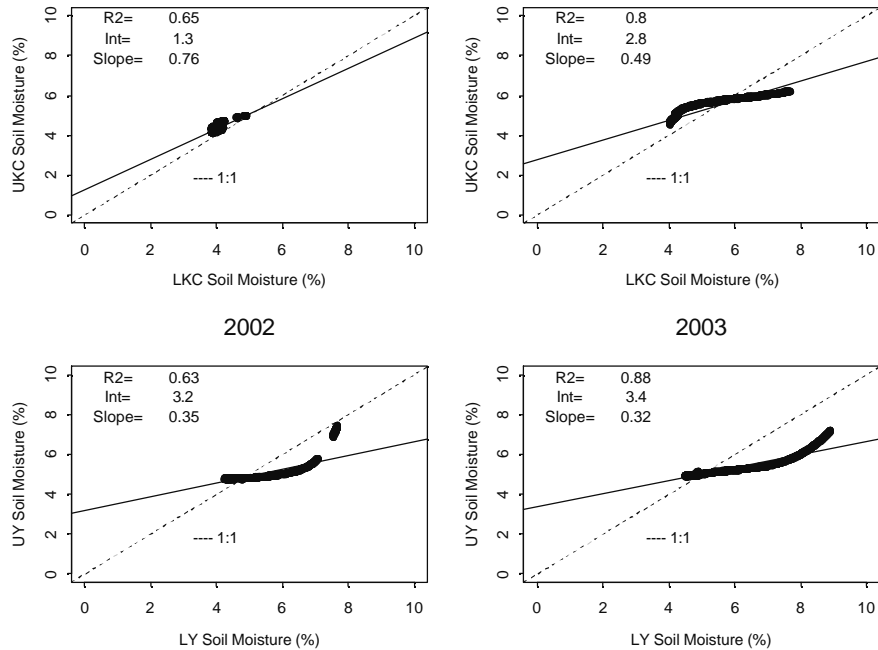
Figure 6. Soil moisture at the sites a) over the one and a half-year measurement period, showing seasonal variation, and b) Comparisons between upslope dry sites and mesic riparian sites.
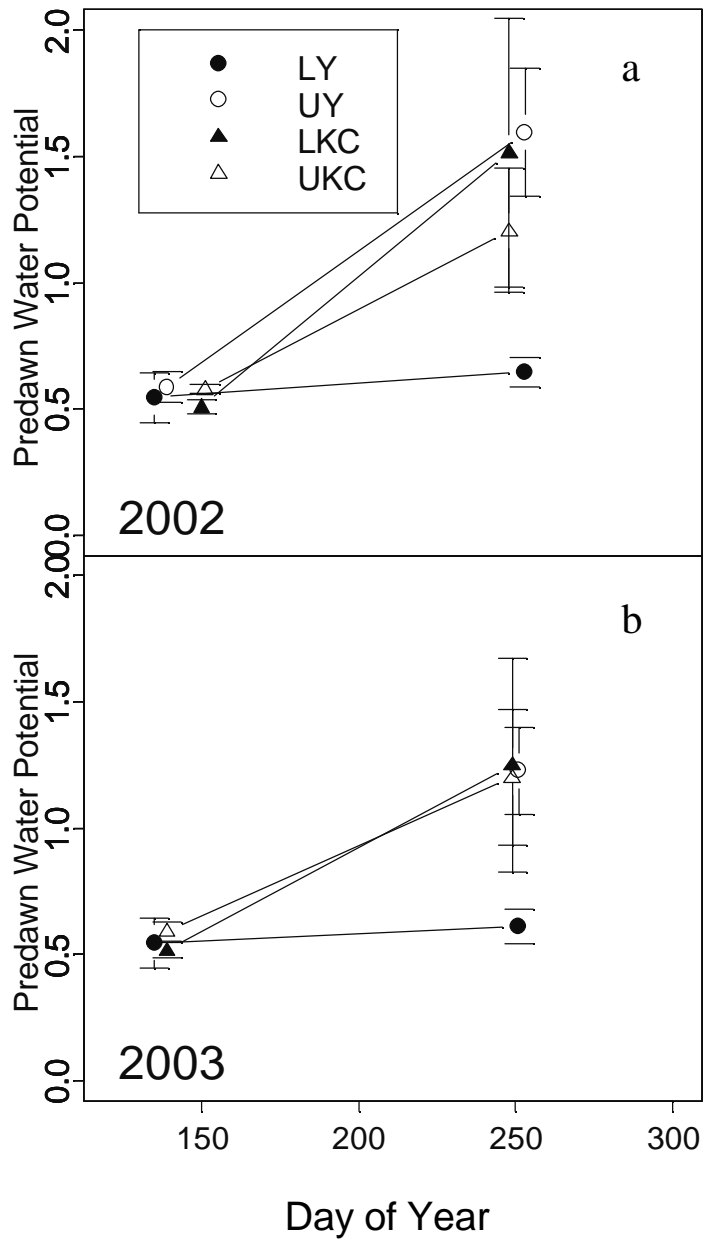
Figure 7. Water potential measured in May and September of each year in
2002 (a) and 2003 (b). LY=Lower Yosemite, UY=Upper Yosemite,
LKC=Lower King's Canyon, UKC=Upper King's Canyon. Error bars are
± 1 SD.
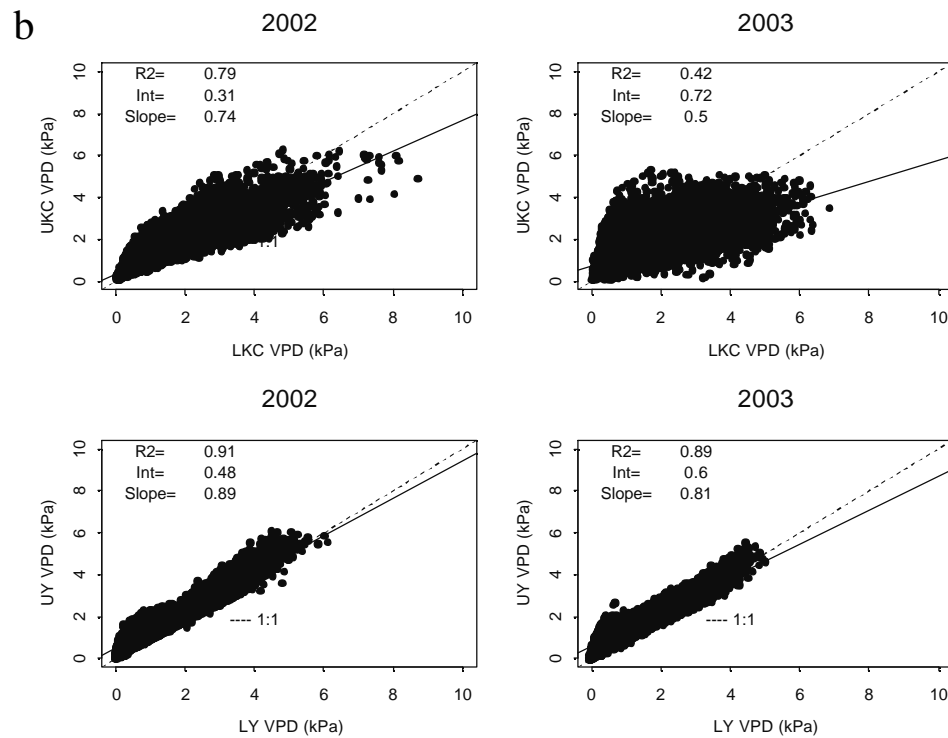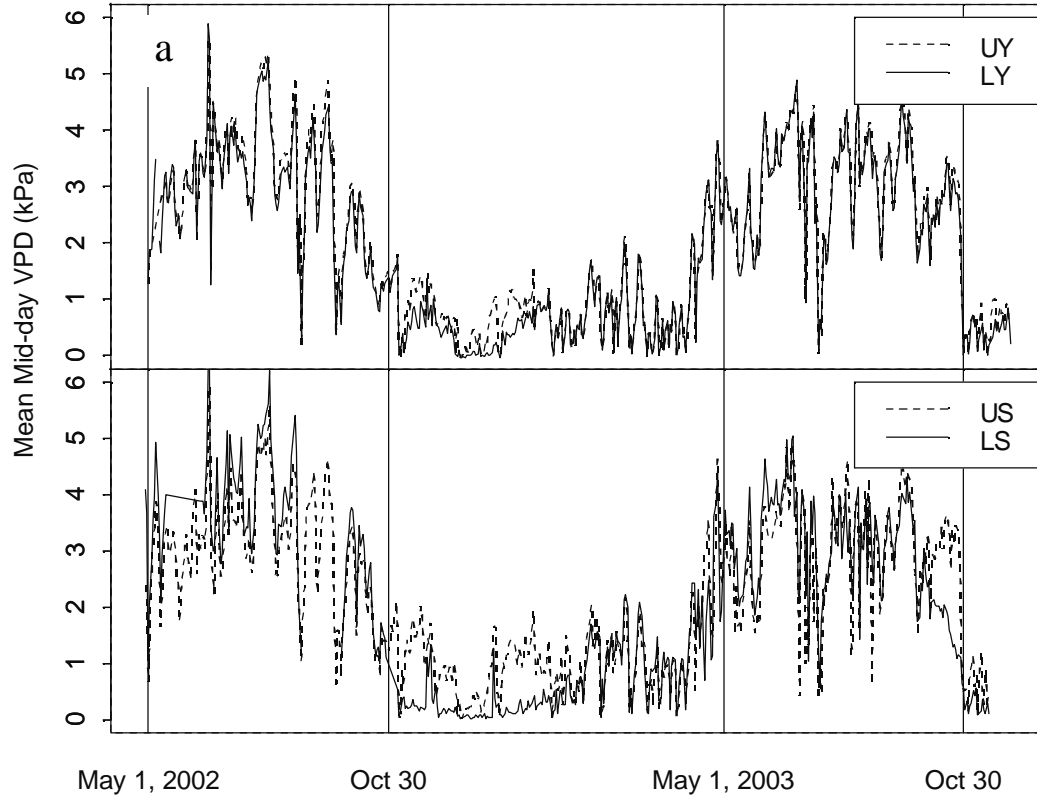
Figure 8. Vapor pressure deficit at the sites a) over the one and a half-year measurement period, showing seasonal variation, and b) Comparisons between upslope dry sites and mesic riparian sites. LY=Lower Yosemite, UY=Upper Yosemite, LKC=Lower King's Canyon, UKC=Upper King's Canyon.
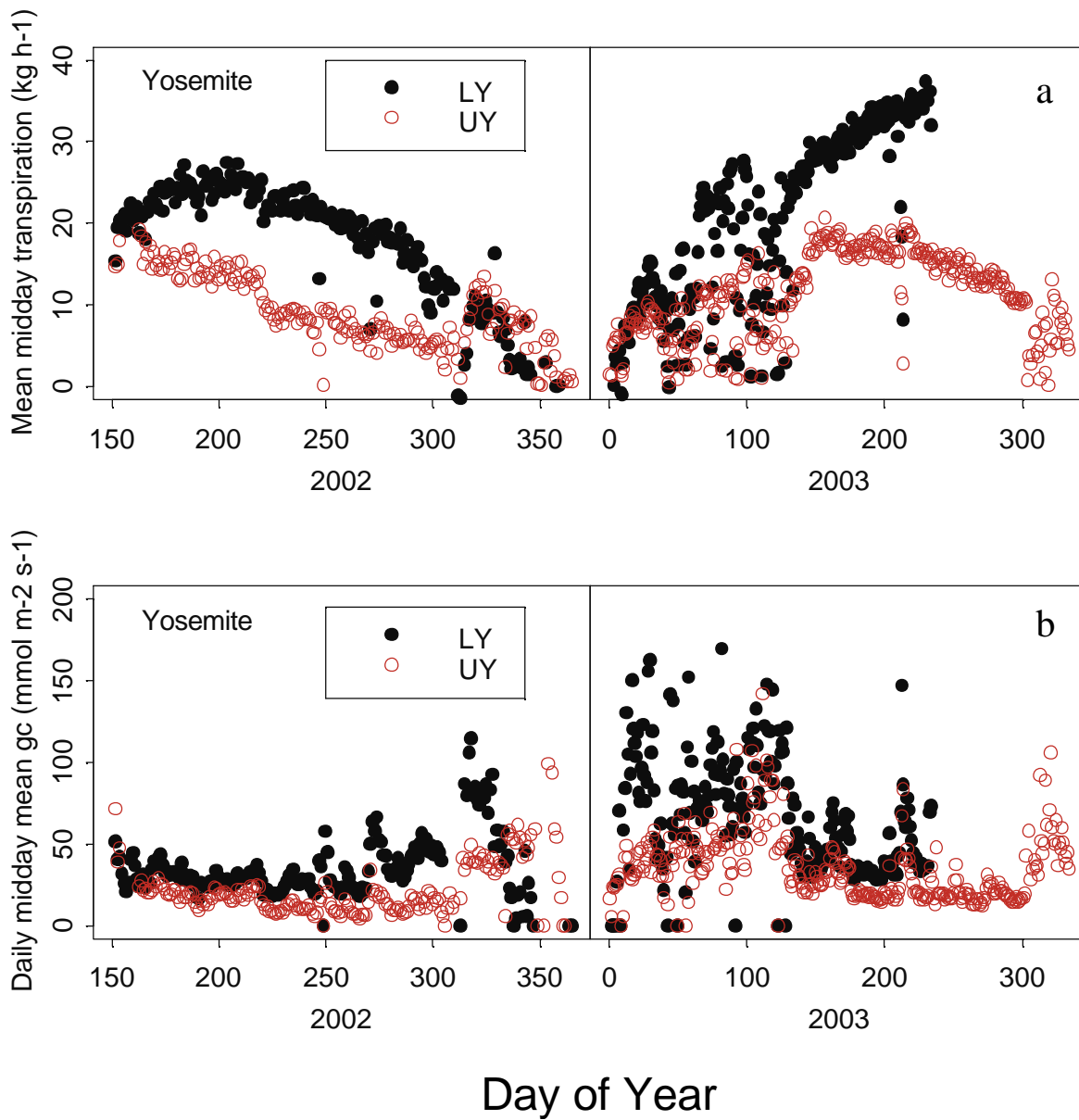
Figure 9. Trends over the study period in mean mid-day (10:00 – 14:00 PST) transpiration (a) and canopy stomatal conductance (b) at the Yosemite sites. LY=Lower Yosemite, UY=Upper Yosemite.

2002

2003

UKC gc (kPa)

200
150
100
50
0

R2= 0.19
Int= 17
Slope=0.29

a

---- 1:1

0   50   100   150   200

LKC gc (kPa)

LKC gc (kPa)

UKC gc (kPa)

2002

2003

UY gc (kPa)

200
150
100
50
0

R2= 0.19
Int= 17
Slope=0.29

b

---- 1:1

0   50   100   150   200

LY gc (kPa)

UY gc (kPa)

200
150
100
50
0

R2= 0.36
Int= 13
Slope=0.25

c

---- 1:1

0   50   100   150   200

LY gc (kPa)
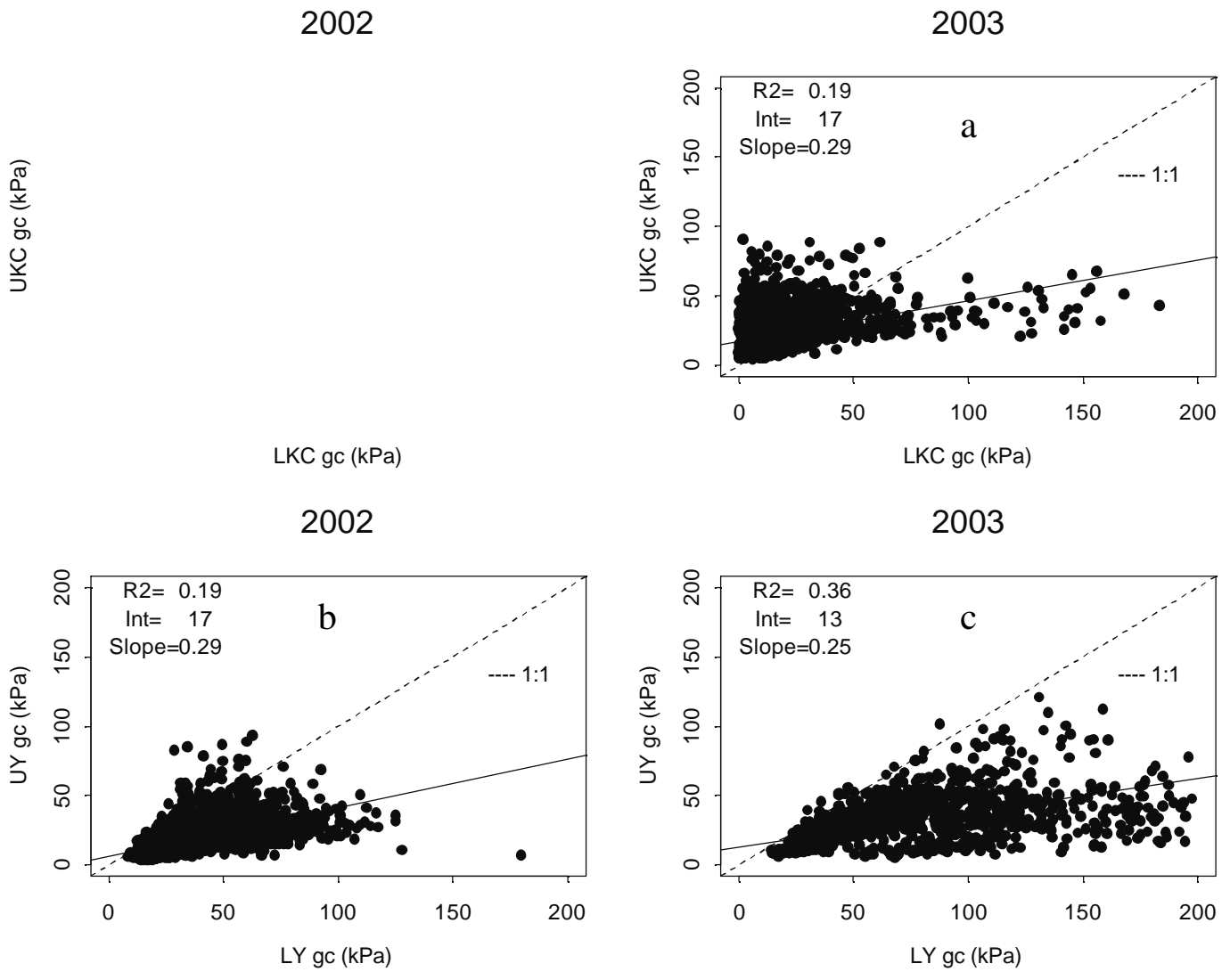
Figure 10. Comparisons of canopy stomatal conductance between upper and lower sites at King's Canyon (a), at Yosemite in 2002 (b) and Yosemite in 2003 (c). The first panel is blank because the lower King's Canyon site wasn't operational until November 2002.
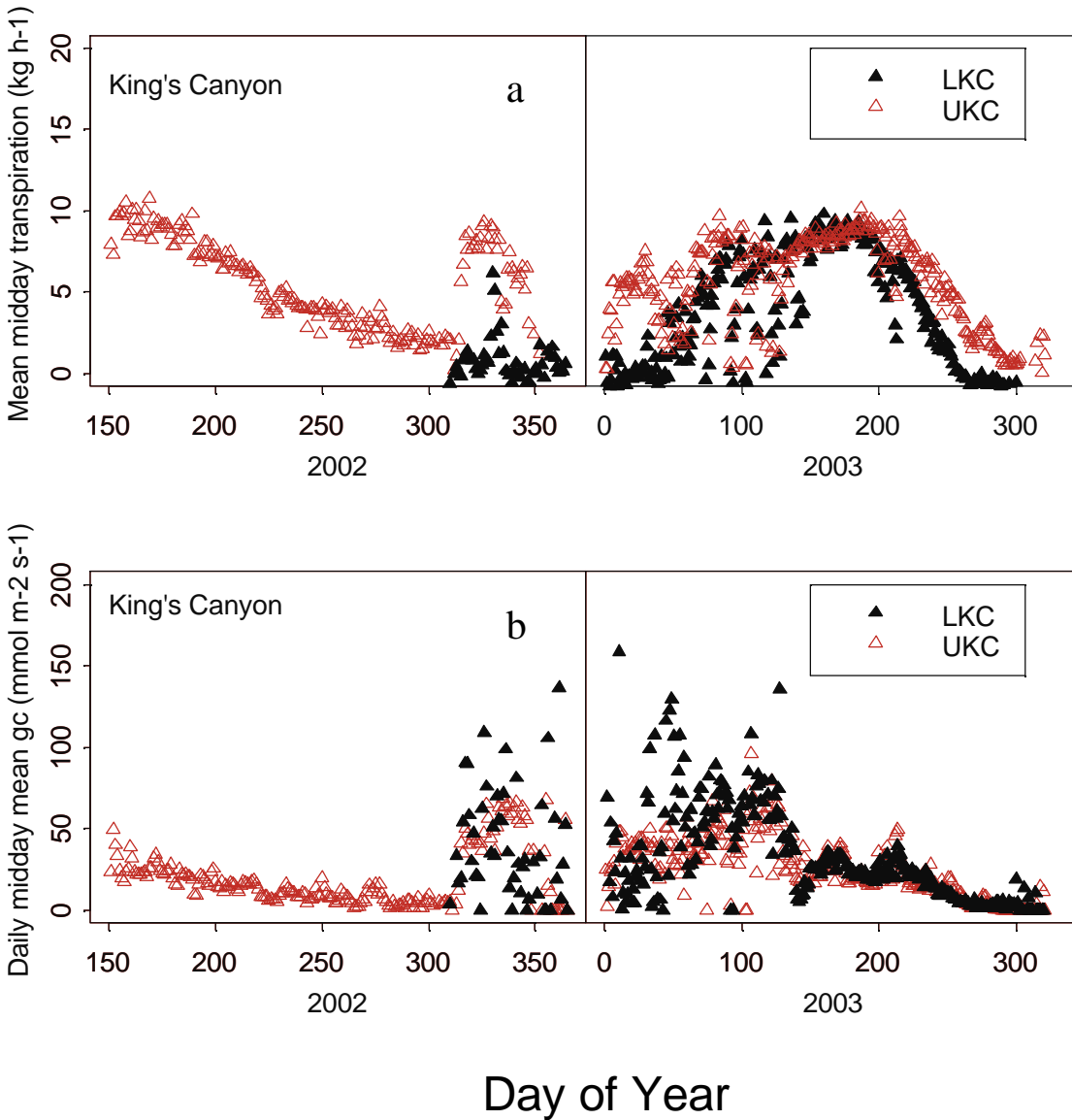
Figure 11. Trends over the study period in mean mid-day (10:00 – 14:00 PST) transpiration (a) and canopy stomatal conductance (b) at the King's Canyon sites. LKC=Lower King's Canyon, UKC=Upper King's Canyon.
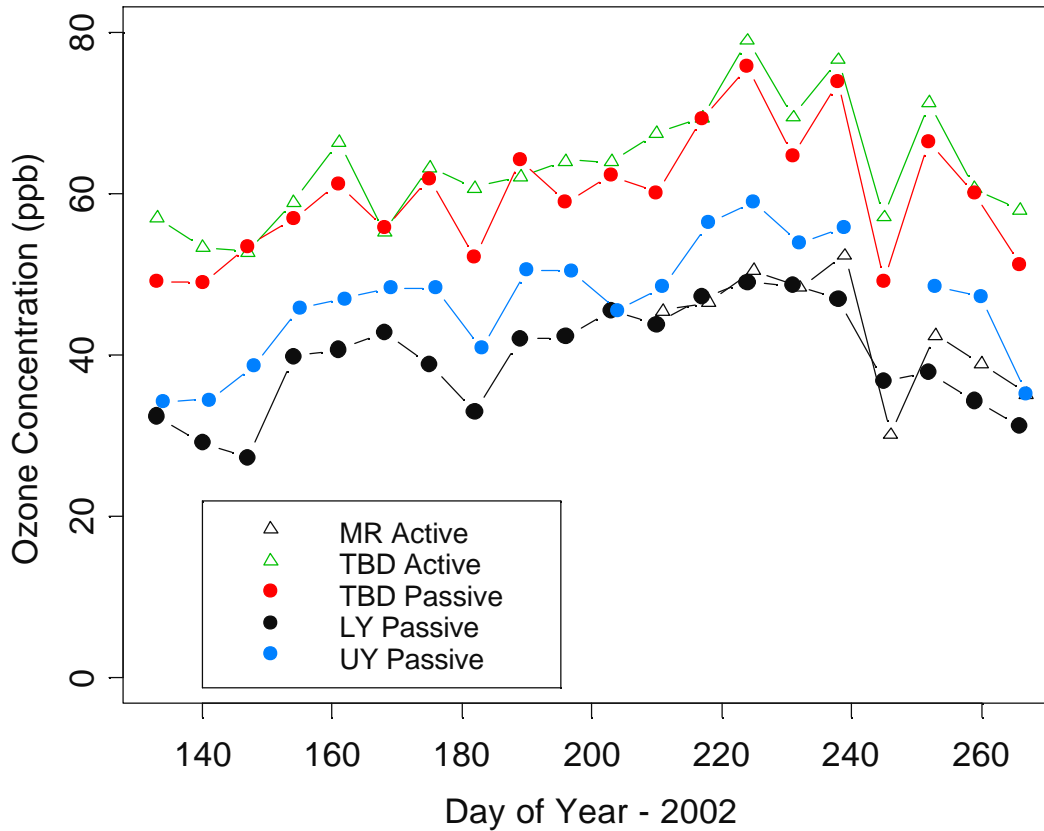
Figure 12. Trends from May – September 2002 in passive ozone monitors (circles) located at the upper and lower Yosemite sites, and co-located active ozone monitors (triangles) at Merced River (MR) and Turtleback Dome (TBD). The relationship between the upper and lower site passives had R^2=0.8, slope = 0.97, intercept=8.5. Upper site ozone concentration was also highly correlated with ozone concentration at the Turtleback Dome site (R^2=0.85, slope = 0.86, intercept = -6.0). The relationship between the Merced River passive and active had R^2=0.74, slope=0.79 and intercept=7.5. These relationships were used to fill in gaps in the ozone data. See text.
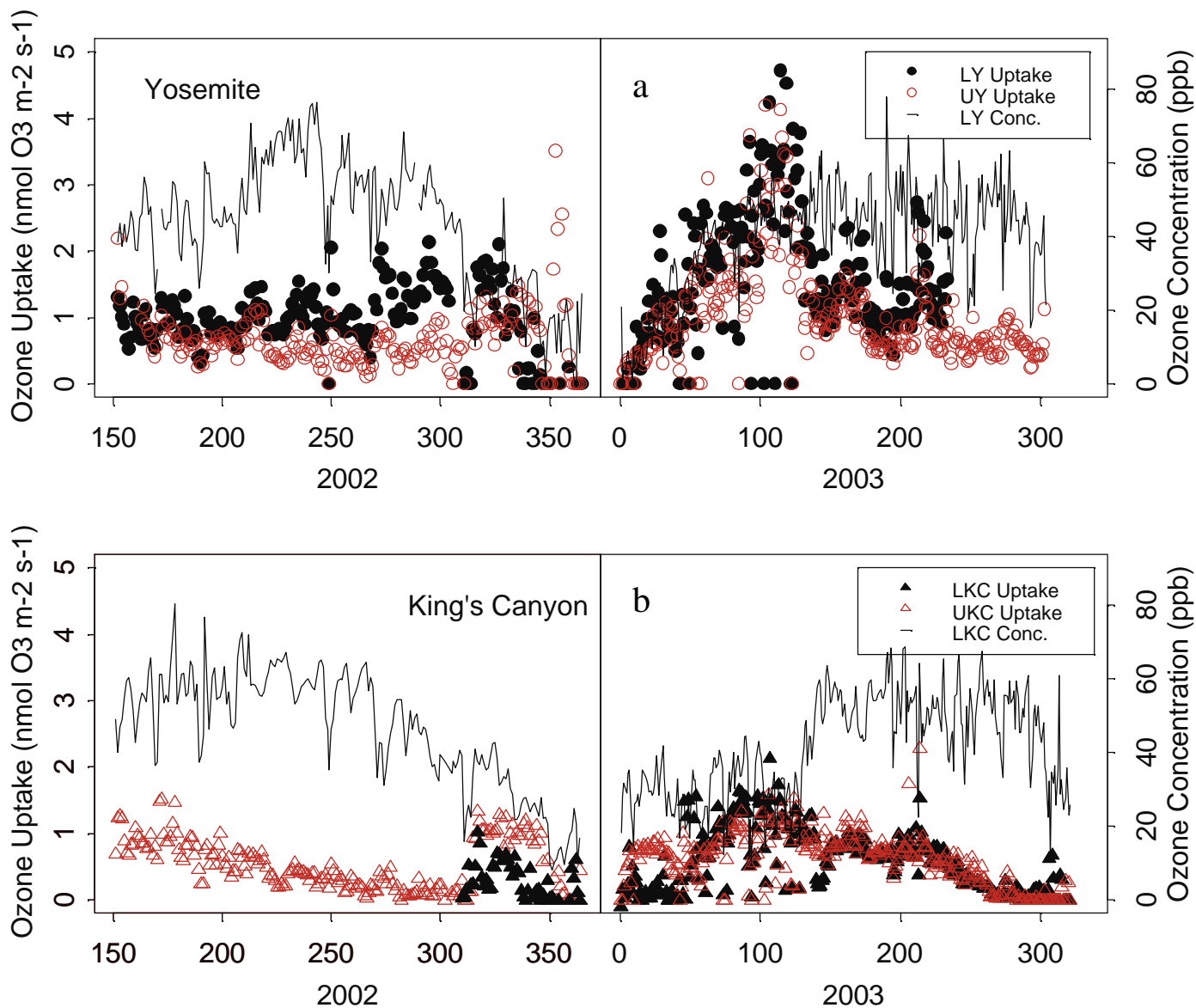
Figure 13. Mean mid-day (10:00 – 14:00 PST) ozone uptake and concentration trends over the study period in at the Yosemite sites (a) and the King's Canyon sites (b). Note the high ozone concentrations over the summer months, but the decreasing trend in ozone uptake in response to decreasing stomatal conductance, despite high concentrations. LY=Lower Yosemite, UY=Upper Yosemite, LKC=Lower King's Canyon, UKC=Upper King's Canyon.
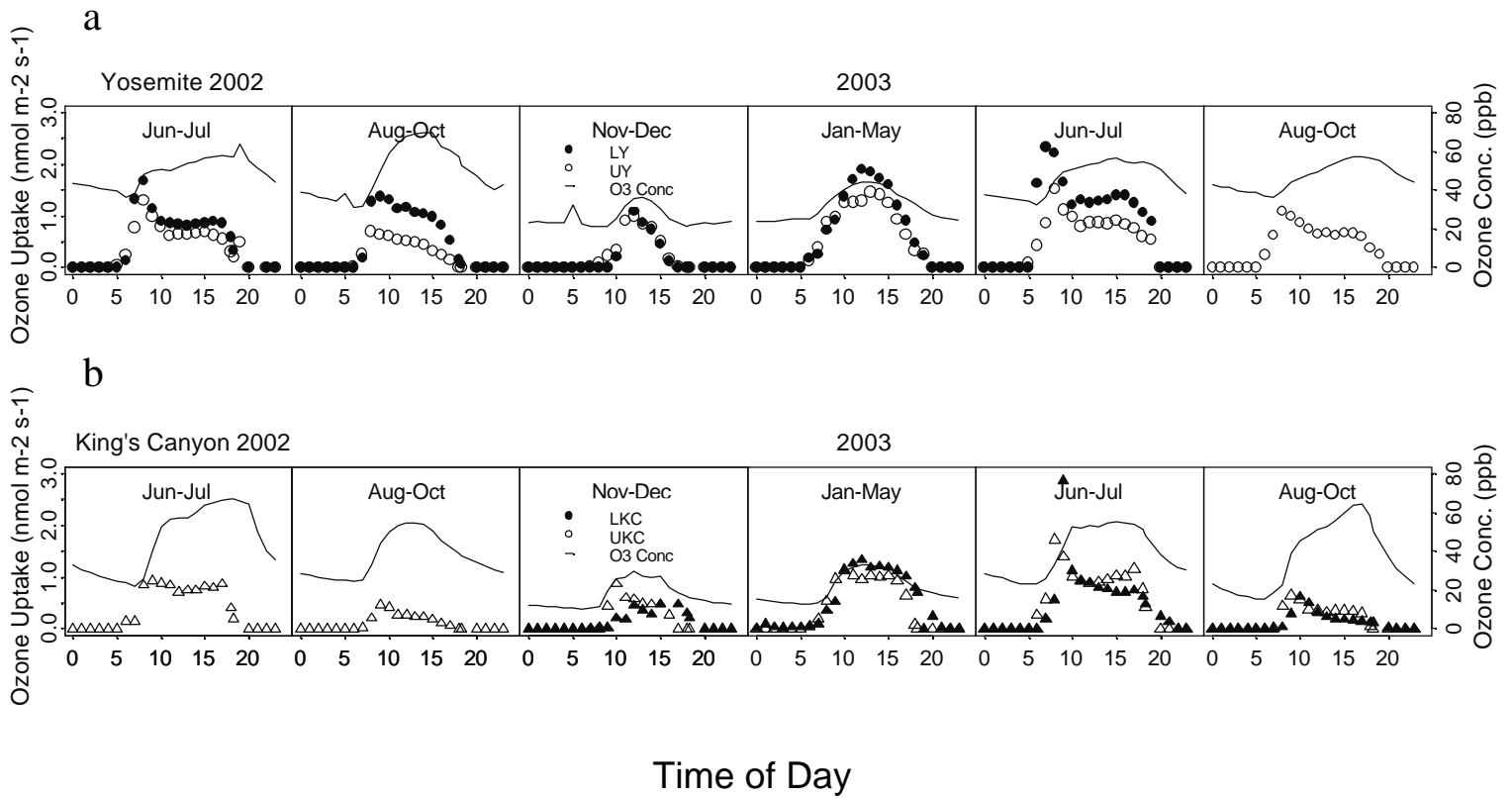
Figure 14. Diurnal patterns in ozone uptake and concentration averaged over periods representing temporal moisture regimes in Yosemite (a) and King's Canyon (b). June-July is a summer warm and wet period, August-October is a warm and dry period, November-December is wet and generally cold, January-May is wet and of variable temperature. Note that the upper Yosemite site diverges below the lower site under the moisture stress of the August-October period, but the sites are nearly identical in the warm, wet June-July period.
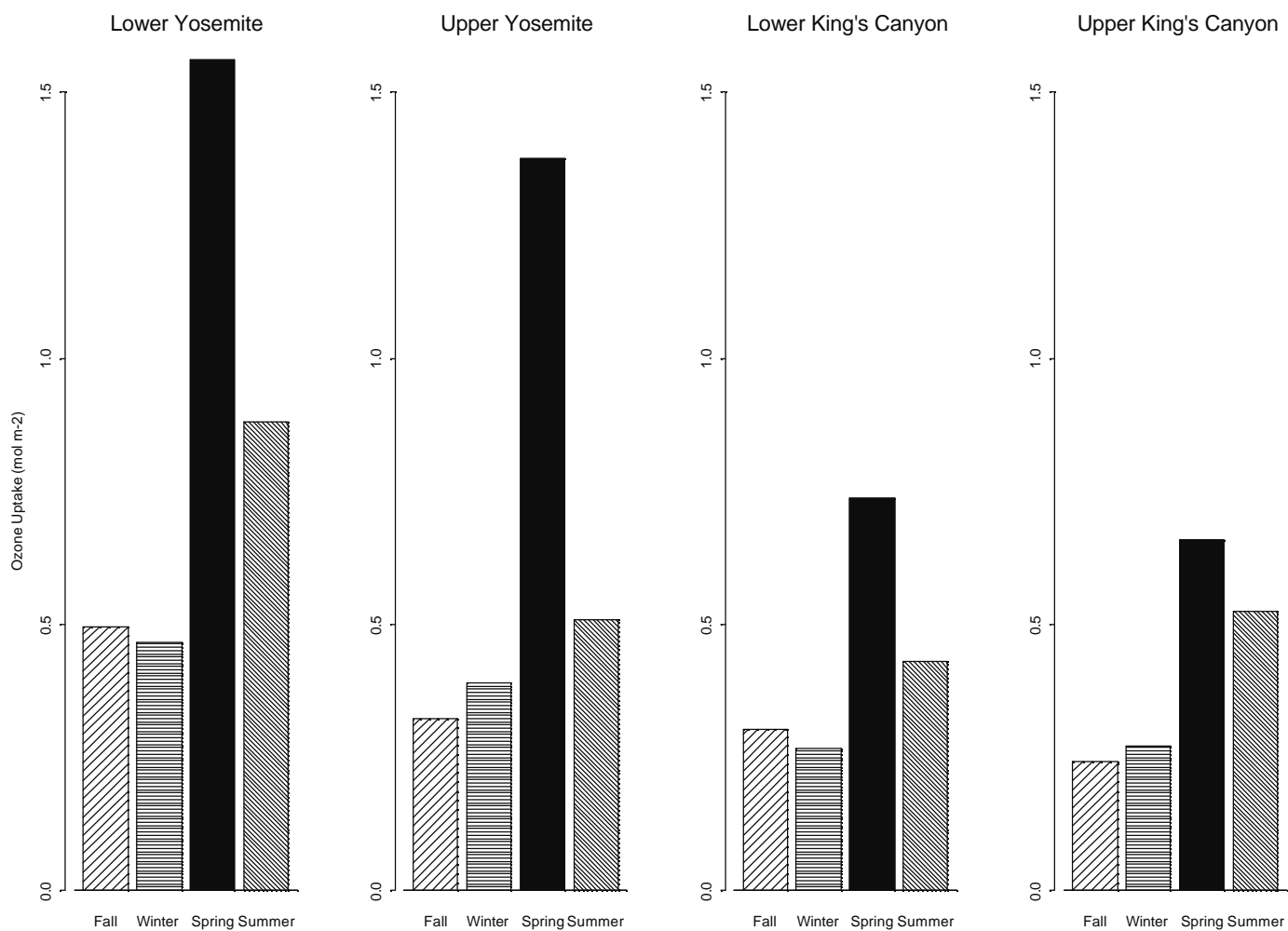
Figure 15. Ozone uptake (mol m^{-2}) summaries by season at the different sites. Seasons are divided conventionally. Fall is September 21 – December 21, Winter: December 22 – March 21, Spring: March 22 – June 21, Summer: June 22 – September 21.

King's Canyon

Yosemite
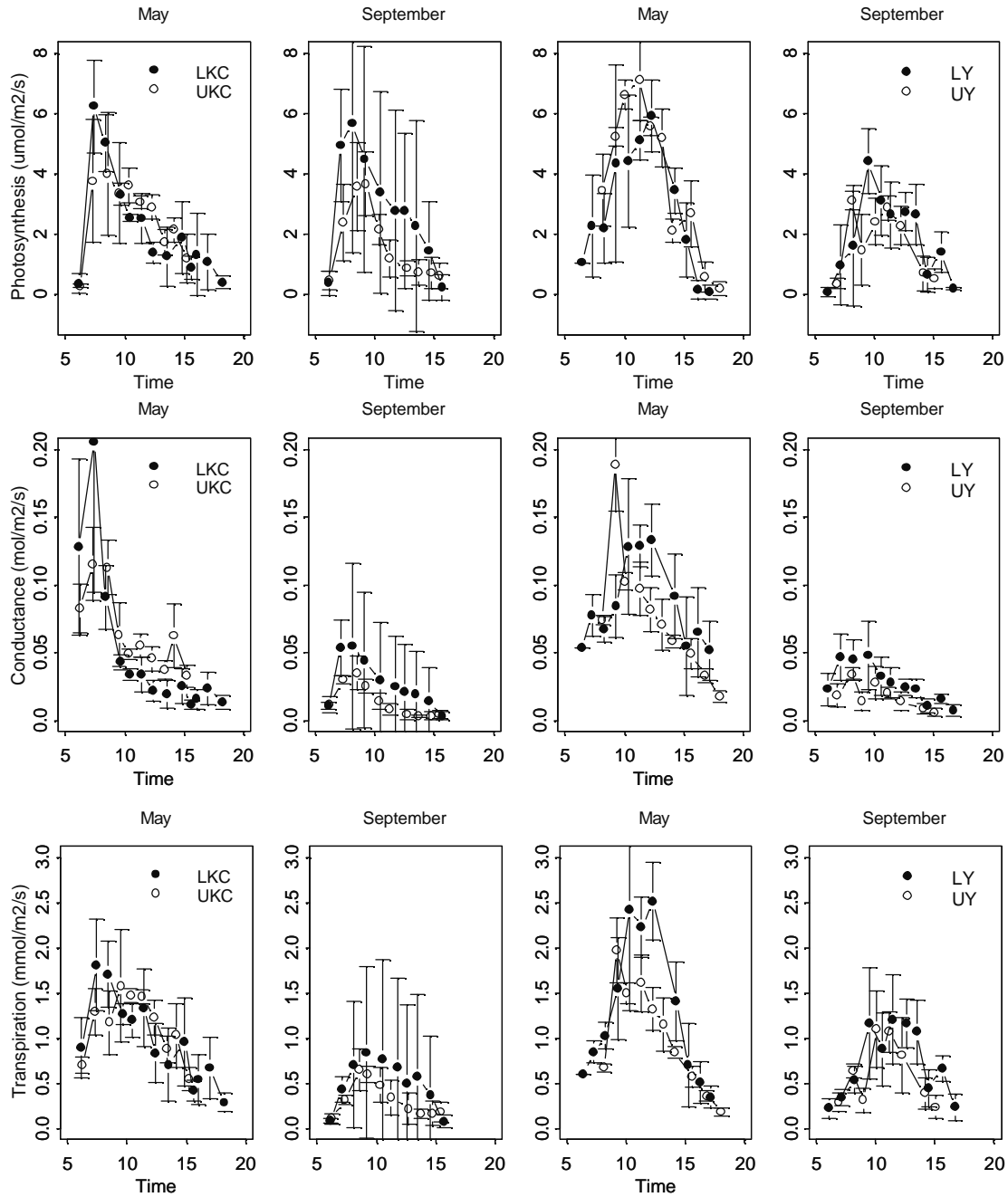
Figure 16. Leaf level physiology measured over a one-day period on one south-facing branch of three trees at all the sites, once in May and once in September, 2002. Error bars are ± 1 SD.
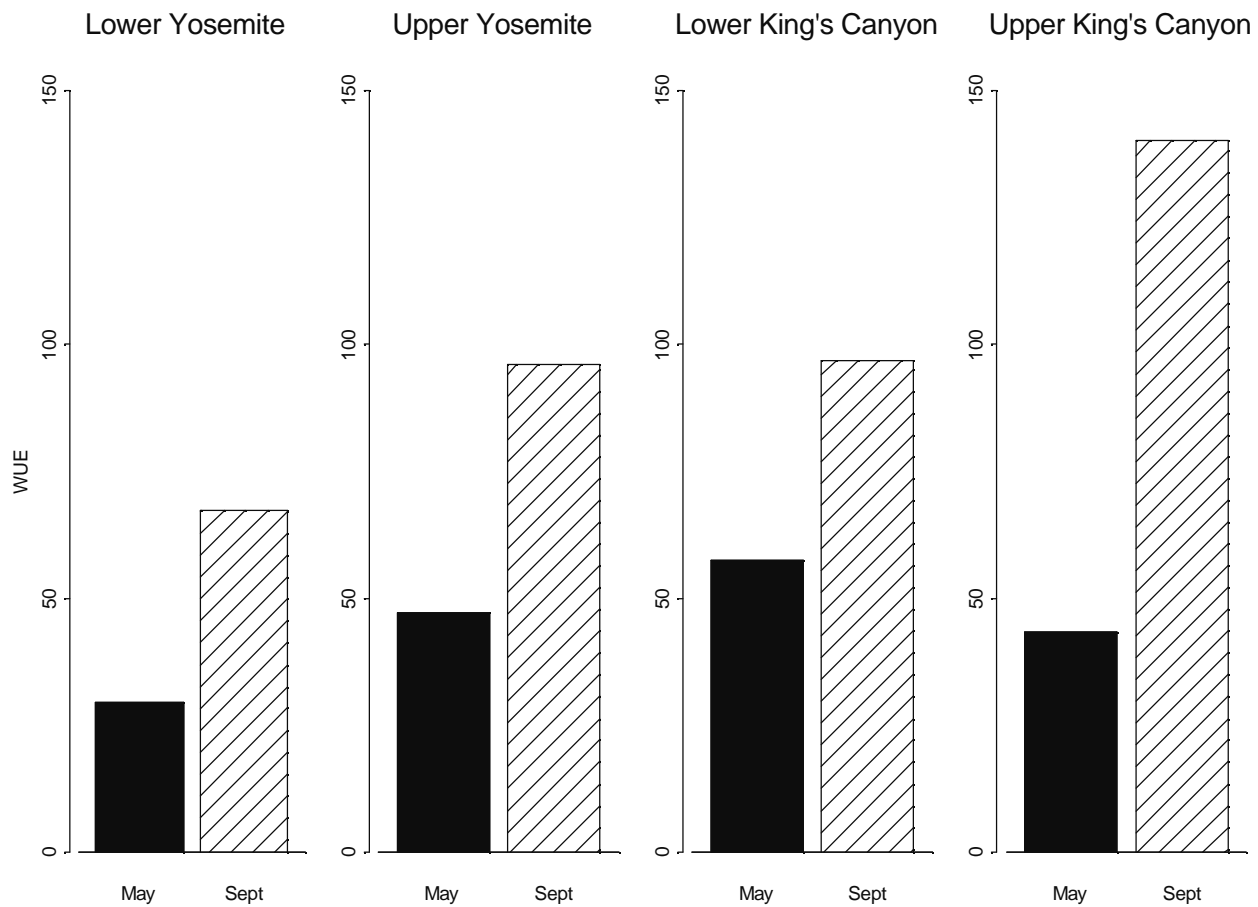
Figure 17. Instantaneous water-use efficiency (WUE), measured as net photosynthesis (μmol m^{-2} s^{-1})/stomatal conductance (mol m^{-2} s^{-1}) using leaf-level data. All differences between May and September significant at the P<0.01 level.
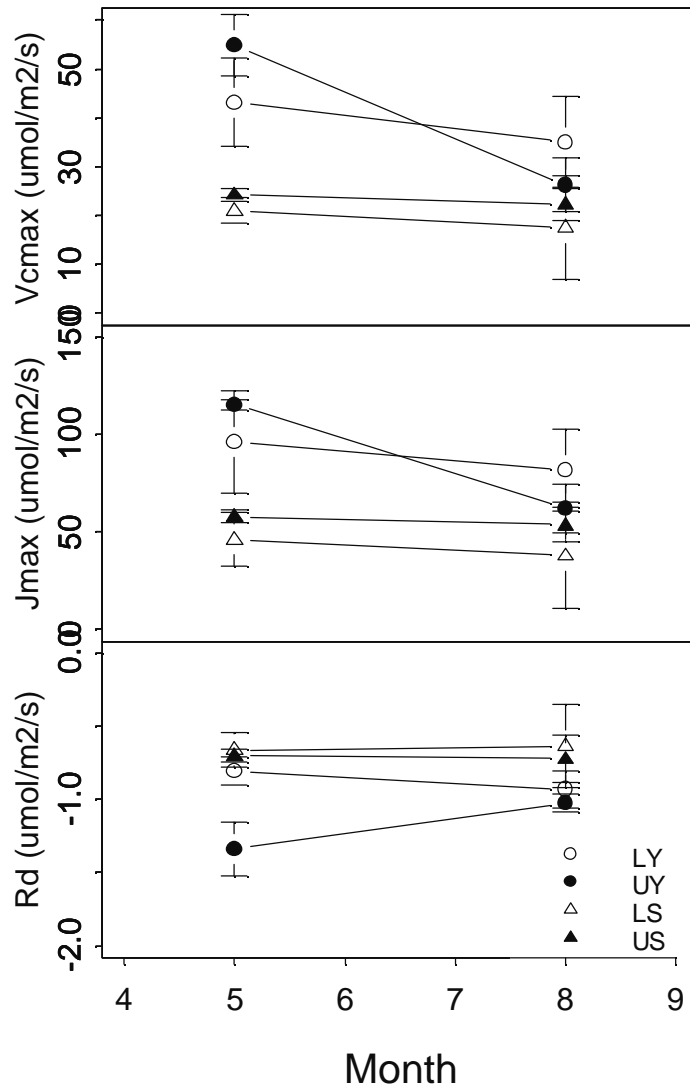
Figure 18. Results from A/C$_i$ curve analyses, measured in May and September at the leaf-level on one south-facing branch of three trees at each of the sites. The only significant difference between May and September is at the upper Yosemite site ($P<0.05$). Error bars are $\pm$ 1 SD. These results were used for the parameterizing STOMATA, the physiological model developed for pine in the Sierra Nevada.
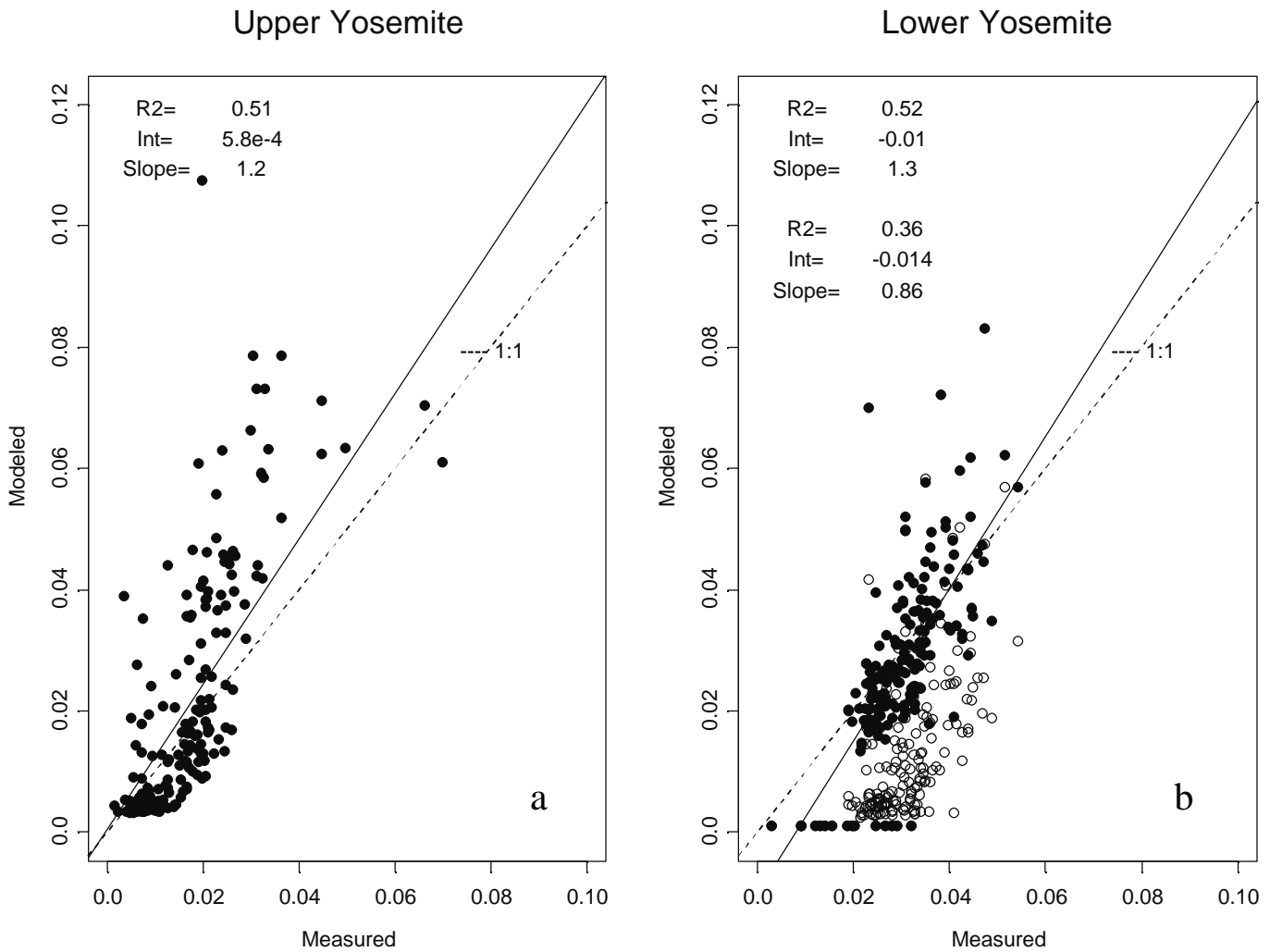
Figure 19. Results from STOMATA at the Yosemite sites. STOMATA predicted stomatal conductance adequately at the Upper Yosemite site (a). At the lower Yosemite site (b) results are shown with soil moisture unmodified (open circles, R^2=0.36), and modified to better represent tree-available soil moisture (solid circles, R^2=0.52).

Lower Yosemite 2002
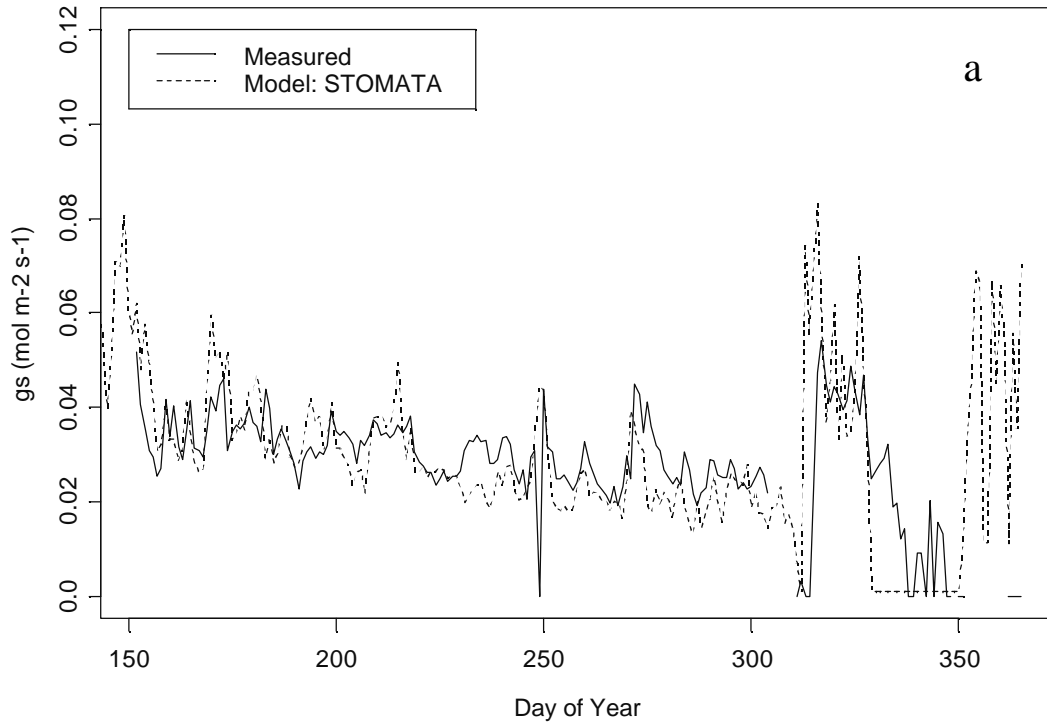
Upper Yosemite 2002
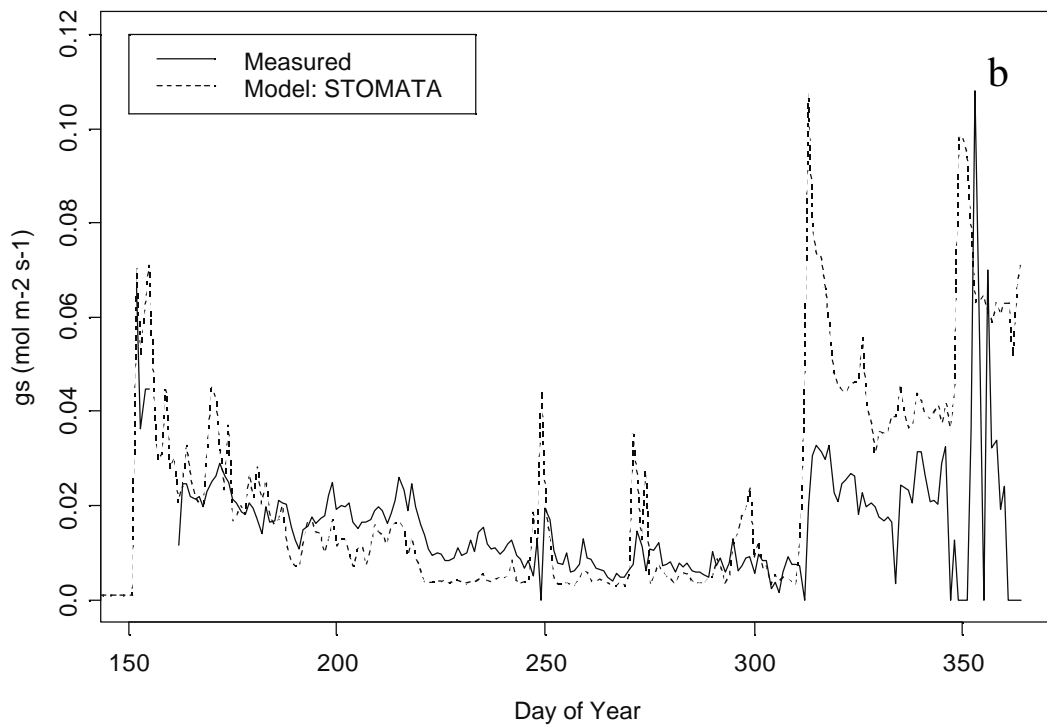
Figure 20. Model results compared to measured stomatal conductance in 2002, at the lower Yosemite site (a) and upper Yosemite site (b).
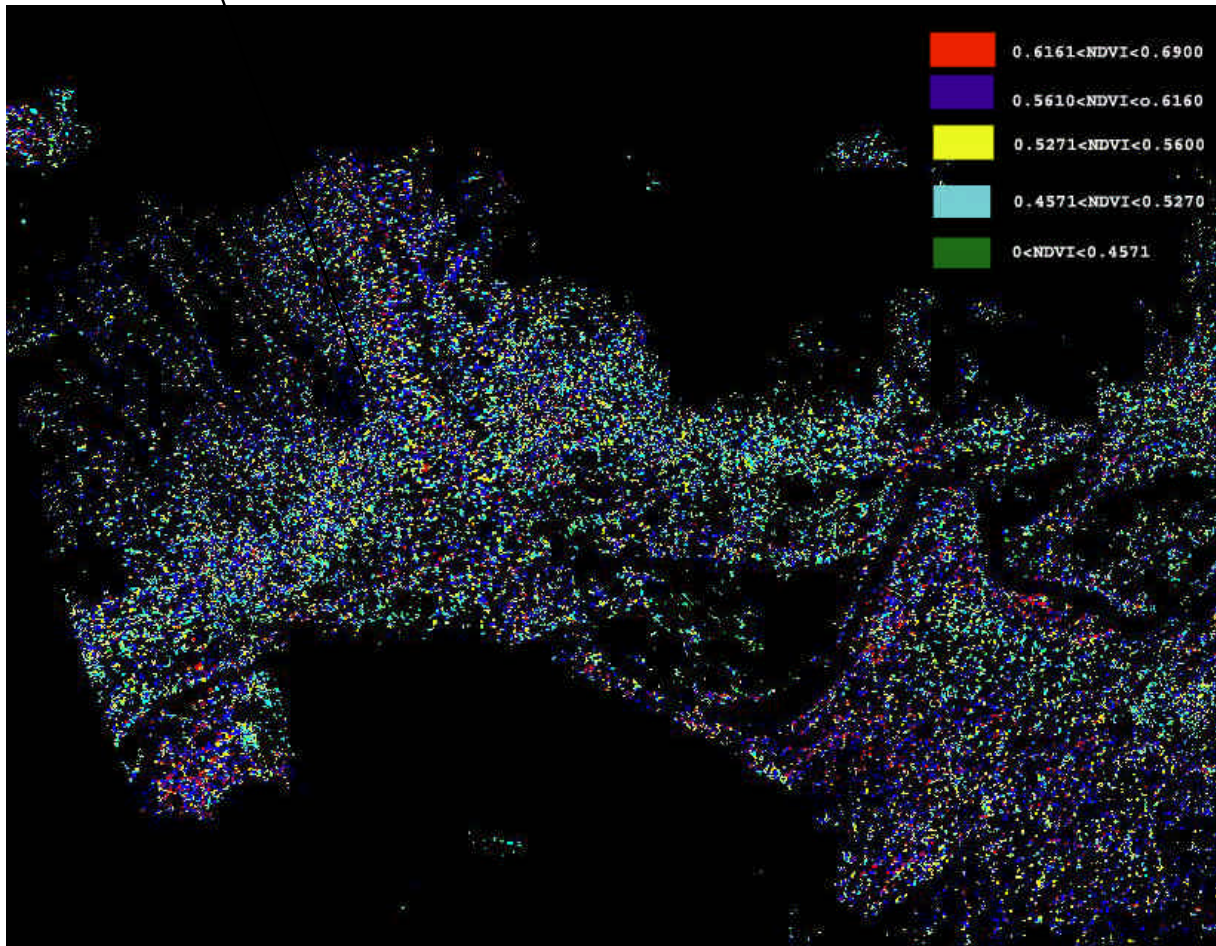
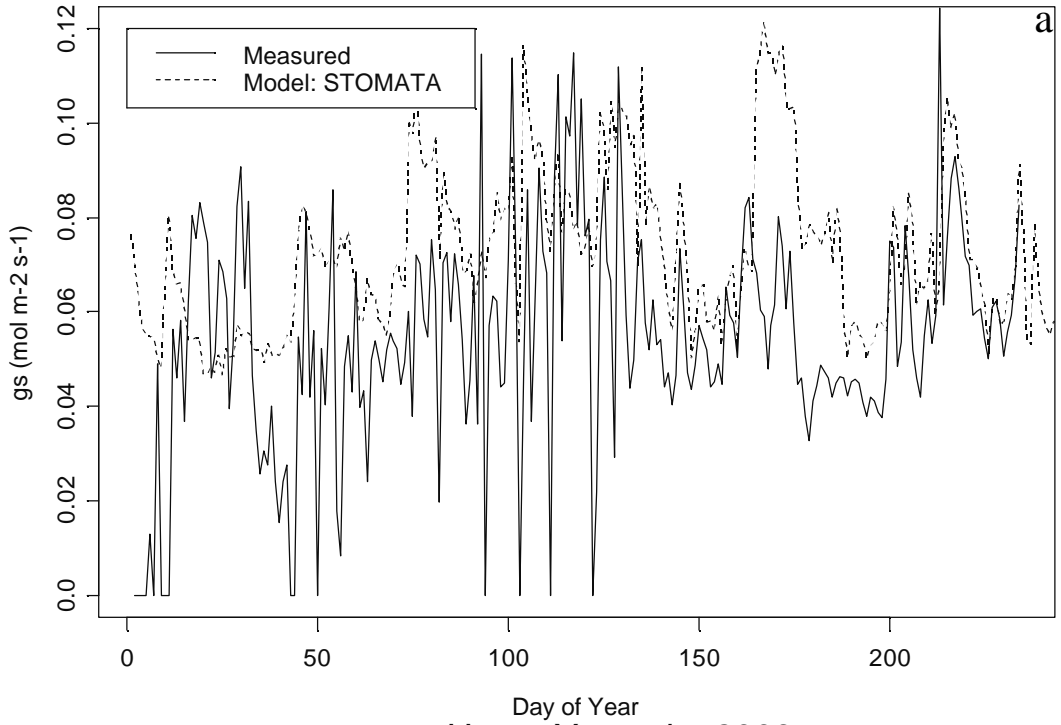**Figure 21: Subset of the NDVI image relative to Yosemite study area**
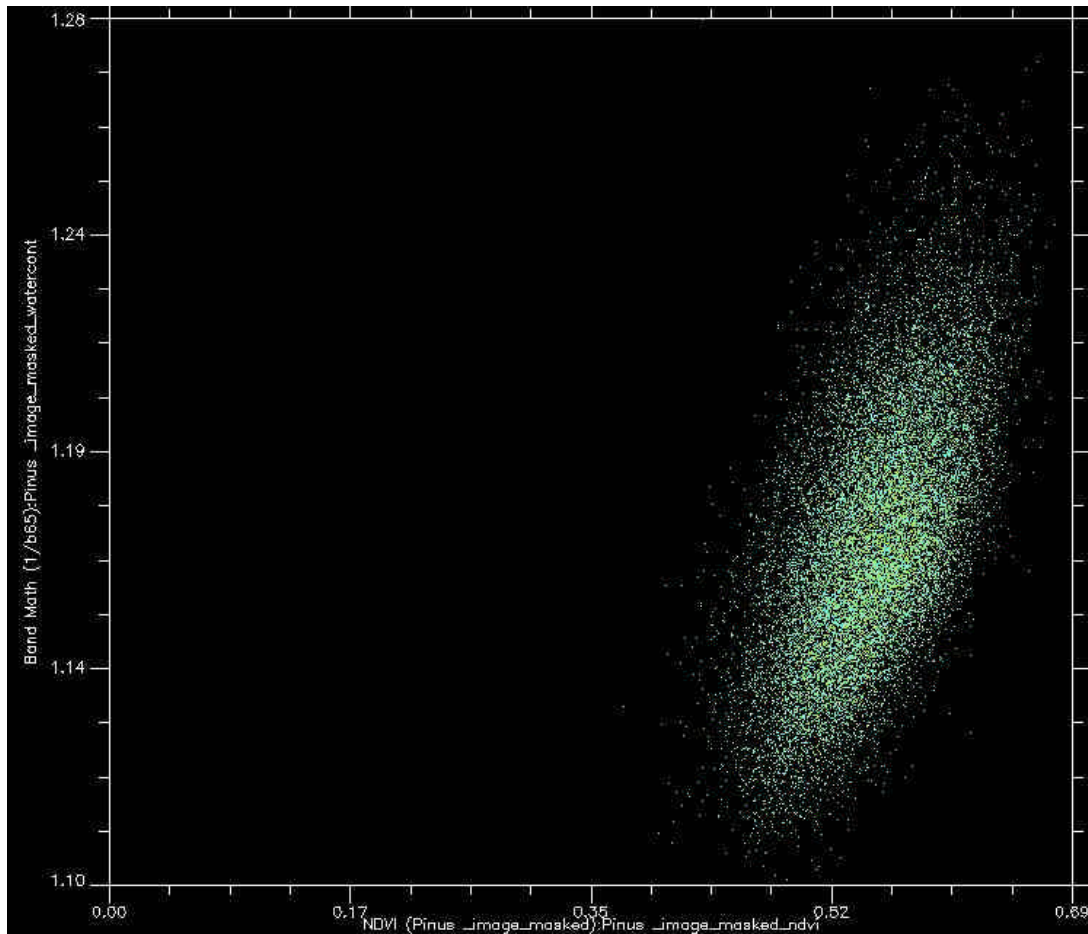
Figure 22: Scatter plot between NDVI and crown water content related to a part of the Yosemite image.

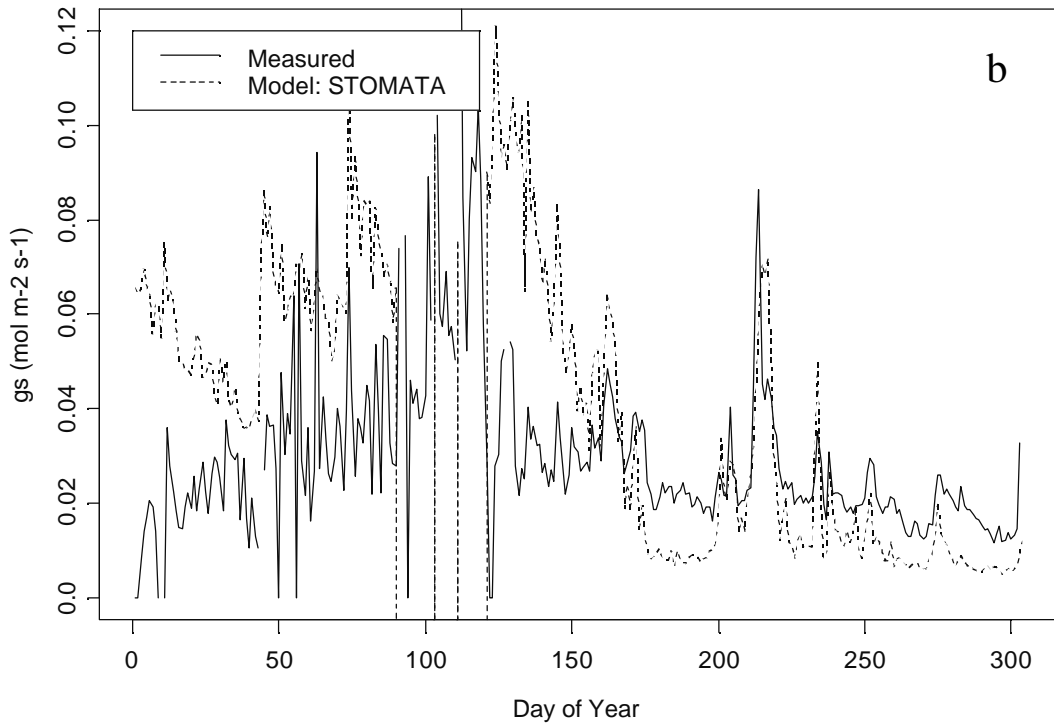## Lower Yosemite 2003
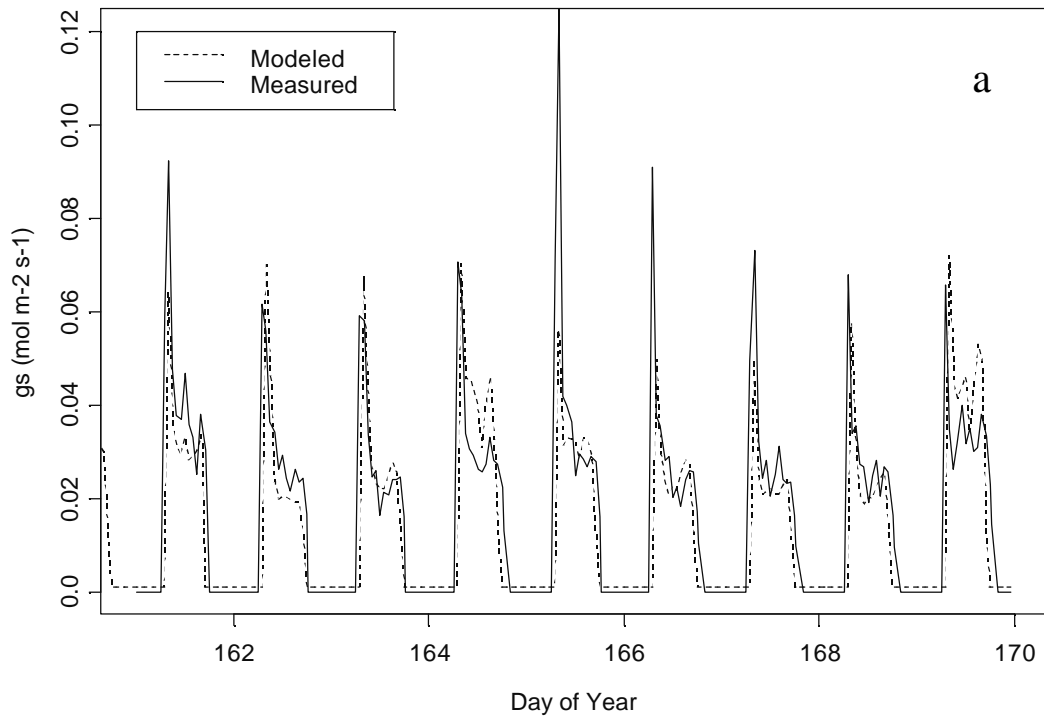

Upper Yosemite 2003

Figure 23. Model results compared to measured stomatal conductance in 2003, at the lower Yosemite site (a) and upper Yosemite site (b).

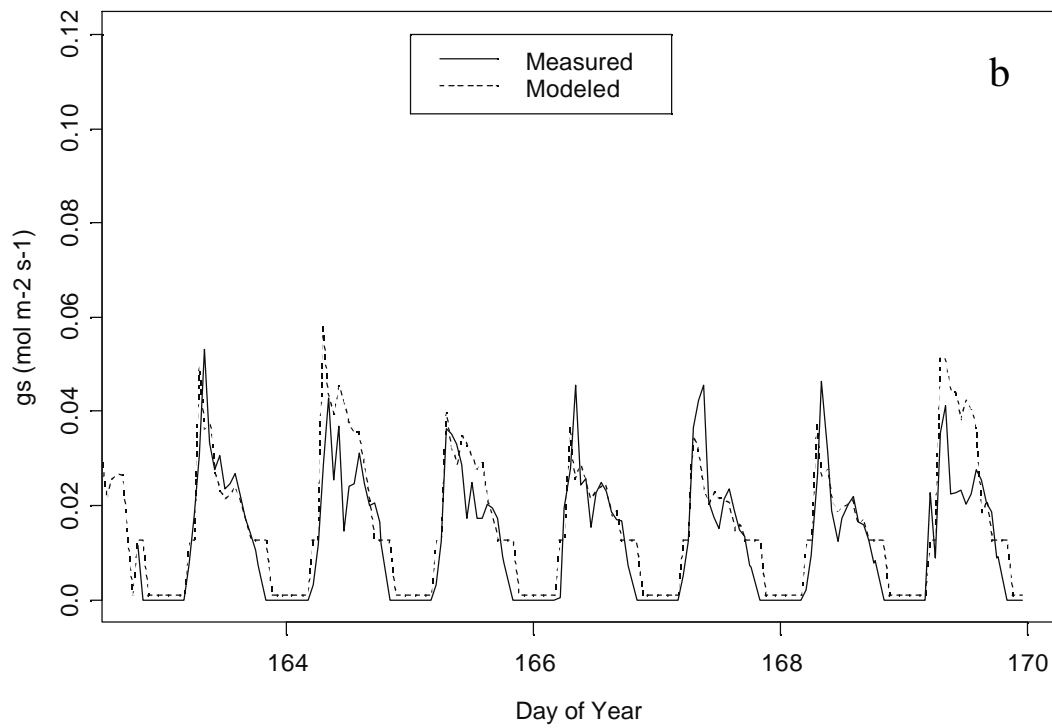## Lower Yosemite 2002

Upper Yosemite 2002

Figure 24. Model results compared to measured stomatal conductance in 2002, at the lower Yosemite site (a) and upper Yosemite site (b), using an early summer window of days to show model performance with diurnal patterns of stomatal conductance.